Ab initio calculation of molecular energies including parity violating interactions

Ayaz Bakasov, Tae-Kyu Ha, and Martin Quack[a)]
Laboratorium für Physikalische Chemie, ETH-Zürich (Zentrum), CH-8092 Zürich, Switzerland

(Received 5 February 1998; accepted 19 May 1998)

We present a new approach towards electroweak quantum chemistry including the parity violating weak nuclear force. After introducing the ground work of electroweak quantum chemical perturbation theory to calculate parity violating potentials, E_{pv}, we present specifically a CIS-RHF method (configuration interaction singles—restricted Hartree–Fock). The method is compared to the previously established and widely used SDE-RHF method for calculations of E_{pv} [single determinant excitations—restricted Hartree–Fock, R. A. Hegstrom, D. W. Rein, and P. G. H. Sandars, J. Chem. Phys. **73**, 2329 (1980)]. It is demonstrated that the new CIS-RHF method can lead to values of E_{pv} which are more than an order of magnitude larger than those obtained with SDE-RHF (for example in H_2O_2, where the new maximum value is $E_{\mathrm{pv}}=3.7\times10^{-19}E_h$). Furthermore, the importance of the tensor character of E_{pv} is outlined by showing that the components of the trace of this tensor $E_{\mathrm{pv}}^{xx}+E_{\mathrm{pv}}^{yy}+E_{\mathrm{pv}}^{zz}=E_{\mathrm{pv}}$ evolve essentially independently from each other in magnitude and sign as functions of molecular structure and computational method. The total E_{pv} results thus as a remainder after substantial mutual cancellation of these components. This finding explains the phenomenon of zero total E_{pv} at chiral geometries, whereas the individual tensor components remain nonzero. We present systematic investigations of parity violating potentials as a function of structure for H_2O_2, H_2S_2, N_2O_4, C_2H_2, C_2H_4, C_2H_6, CH_4, and alanine. The effect of nuclear charge Z is investigated for the pair H_2O_2 and H_2S_2 and a power law $Z^{3+\delta}$ ($\delta\approx1.5$) for the enhancement of E_{pv}^{ii} can be established with significance for the individual tensor components ($i=x,y$, or z), whereas just considering the total E_{pv} would be misleading in analyzing the Z dependence. Contributions of hydrogen atoms to E_{pv} are estimated and found to be orders of magnitude lower than those of the heavier atoms mentioned. The results are discussed in relation to a possible spectroscopic experiment to measure $\Delta E_{\mathrm{pv}}=2E_{\mathrm{pv}}$ in enantiomers of chiral molecules and in relation to various hypotheses for the origin of nature of homochirality in chemical evolution.
 [S0021-9606(98)30332-3]

I. INTRODUCTION

The traditional quantum chemical treatment of molecular energies, including chiral molecules, uses a Hamiltonian which is invariant under inversion of all particle coordinates in the center of mass and thus conserves the quantum number parity.[1] An immediate consequence for chiral molecules would be that eigenstates of the molecular Hamiltonian would possess a well-defined parity, and time-dependent states would conserve parity in time, if it is well defined initially. Such states will not be chiral. One may nevertheless define chiral molecular states with time dependence due to tunneling processes, which are so slow that they can be neglected on ordinary times scales of chemistry. This idea was, indeed, at the origin of the first quantum-mechanical theory of chiral molecules.[1] The situation changed drastically with the discovery of parity violation in weak nuclear interactions.[2,3] With the subsequent formulation of electroweak theory,[4–6] it would seem natural to include parity violating forces in quantum chemical calculations, however, it turns out that the corresponding parity violating molecular potentials are so small (of the order of $10^{-15(\pm3)}$ J mol^{-1} for the lighter elements) that they can usually be safely neglected. Chiral molecules form an obvious exception, due to the close degeneracy of states of different parity. It has thus been noted more than two decades ago that a correct physical–chemical treatment of chiral molecules should include the parity violating effective potentials.[7–11] Particularly following the work of Hegstrom *et al.* in 1980,[12] there have been several quantitative calculations, largely on the basis of their SCF (self-consistent field) theory formulation, for parity violating potentials in chiral molecules,[13–32] but also following slightly different lines, using a relativistically parametrized extended Hückel method[33–35] (see also the relativistic theory of Abdus Salam,[36,37] which considers phase transition to chiral states). It has furthermore been shown that in spite of the small size of the effects involved, a realistic experiment can be designed to measure the consequences arising from the parity violating potentials,[38–40] including tests of fundamental symmetries.[41,42] Nevertheless, the measurement of such small effects in molecules remains difficult and did not exist until today. It would be most important to have calculations as accurate as possible for parity violating po-

[a)]Author to whom correspondence should be addressed. Phone: +41-1-6324421; Fax: +41-1-6321021; electronic mail: Quack@ir.phys.chem.ethz.ch

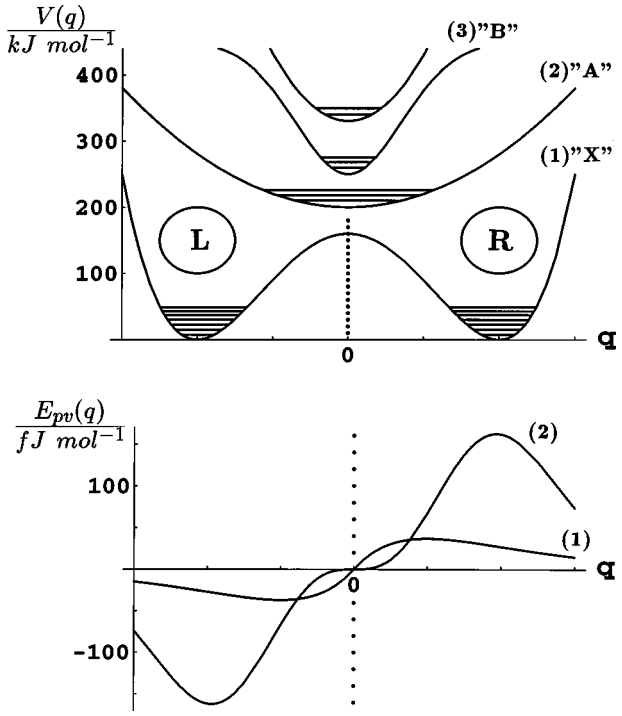

FIG. 1. General illustration for parity conserving and parity violating molecular potentials. The upper part of the figure shows Born–Oppenheimer type (possibly more general) potentials, which are inversion symmetric, separating space along an inversion coordinate q into a ''left-handed'' and a ''right-handed'' part. The ground-state potential ''X'' shown has chiral equilibrium geometries, the excited-state potentials have achiral equilibrium geometries. The lower part of the figure shows the small parity violating potentials for the two lower states (schematic). These should not be naively interpreted as additions to a Born–Oppenheimer potential but are effective potentials of different symmetry.

tentials, both for planning such experiments and for current discussions of the influence of parity violation on chiral discrimination in molecular evolution.[7,30,43–45] For a review of various alternative theories of molecular chirality, including effects from environmental perturbations, we refer to Ref. 39.

The nature of the problem in quantitative calculations of effects from parity violation is schematically illustrated in Fig. 1. One may think here of an inversion coordinate q in the multidimensional space of $3N-6$ internal coordinates for an N atomic molecule, say a substituted amine or methane[46] or a torsional coordinate such as in the example H_2O_2, which we treat quantitatively below. The natural quantum chemical approach is to start out from the Born–Oppenheimer potential or $V(q)$, leading to typical energy differences between different structures and also ground and excited electronic states of the order of a few hundred kJ mol^{-1}. The parity violating potentials $E_{\mathrm{pv}}(q)$ to be derived below are about 18 orders of magnitude smaller, say a few hundred fJ mol^{-1} as also illustrated in the figure. Even the very best quantum chemical calculations for simple molecules today are able to obtain an accuracy of perhaps 1 J mol^{-1}, at which level the breakdown of the Born–Oppenheimer approximation and other small effects become important. It is thus obvious that a calculation of observable molecular quantities arising from parity violation will not pass through a direct calculation of the total potential including parity violation, but rather add the parity violating term as a separate term to the molecular Hamiltonian. Because all other (usually much larger) parts in the molecular Hamiltonian, which are neglected or roughly approximated, are inversion symmetric, one is nevertheless able to calculate meaningful observables arising from $E_{\mathrm{pv}}(q)$ if one concentrates on those measurable quantities which vanish exactly for an inversion symmetric Hamiltonian. For such observables one needs a good, direct calculation of $E_{\mathrm{pv}}(q)$, whereas the absolute, parity conserving potential can be approximated in the normal way at much lower accuracy. Figure 1 illustrates $V(q)$ and such parity violating potentials for a molecule with at least four atoms (say C H F Cl Br), which occurs in left-handed (space L) and right-handed (space R) forms, connected by mirror symmetry. $V(q)$ is rigorously symmetric (to all orders excluding parity violation) around $q=0$ in the one-dimensional representation, whereas E_{pv} is antisymmetric. The weak nuclear interaction can also contribute a parity conserving potential, which is, however, small compared to the uncertainties in other parity conserving molecular potentials and does not contribute to parity violating observables of interest here. At $q=0$ we have an achiral geometry (for instance planar), where E_{pv} vanishes. For each mirror symmetrical pair of left-handed (q_L) and right-handed (q_R) structures,[47] we can define a parity violating energy difference $\Delta E_{\mathrm{pv}}=E_{\mathrm{pv}}(q_R)-E_{\mathrm{pv}}(q_L)$. If the transition states separating the left-handed and right-handed enantiomers are chiral, there exist also enantiomeric transition structures with a corresponding parity violating energy difference. Figure 1 illustrates furthermore the nature of electronic states with minima at the achiral geometry at $q=0$. In the example, these are excited electronic states, but they might of course be also the ground states as in planar polyatomic molecules such as benzene. Even in such achiral electronic states, the parity violating potentials do not vanish for the chiral geometries, and in this sense molecules that are usually considered ''achiral'' are not really different from ''chiral'' molecules with respect to the calculation of $E_{\mathrm{pv}}(q)$. We shall present calculations for both types of molecules below. The difference between chiral and achiral molecules becomes important when we consider quantization of nurovibronic molecular states and of the resulting observables. The usual ordering of electronic (''el''), vibrational (''vib''), rotational (''rot''), and hyperfine (''hfs'') energy spacings is, in particular, for ''achiral molecules'':

$$\Delta E_{\mathrm{el}} \gg \Delta E_{\mathrm{vib}} > \Delta E_{\mathrm{rot}} \gg \Delta E_{\mathrm{hfs}} \gg \Delta E_{\mathrm{pv}}. \tag{1}$$

However, for chiral molecules a special situation arises because of the close degeneracy of the vibrational-tunneling energy levels in the double minimum potential of Fig. 1.[1] There the situation may arise that

$$\Delta E_{\mathrm{vib,tun}} \ll \Delta E_{\mathrm{pv}} \tag{2}$$

and thus the spectroscopically observable effects from parity violation become maximal. Quite generally, parity violating effects in molecular physics will become strongly observable, when for two levels for whatever reason,

$$\Delta E_{\mathrm{el,vib,rot,hfs}} \lesssim \Delta E_{\mathrm{pv}}. \tag{3}$$

Situations where this can arise for both chiral and achiral molecules have been discussed.[38–41] In particular, in such situations, one may find time-dependent nonconservation of the observable ''parity,'' i.e., ''violation'' of parity conservation in molecules due to the parity violating potentials, through which such potentials could be quantitatively measured.[38] This provides at the same time the basis of the nomenclature ''parity violating molecular potentials E_{pv}.''

It has turned out in the course of our investigations that the current methods[12–32] of predicting E_{pv} are quantitatively inadequate. It is thus the goal of our paper to develop routes to improved techniques for the quantum chemical calculations of molecular parity violating potentials.

Anticipating here some of our main results, we have found that the parity violating interaction in molecules has essentially tensor character:

$$E_{\mathrm{pv}}^{i,j}=\sum_{\{n\}} C_{\{n\}}\mathscr{V}^{i}_{\{n\}}\mathscr{A}^{j}_{\{n\}}, \tag{4}$$

where $\mathscr{V}^{i}$ is a component of a polar vector quantity like a momentum operator and $\mathscr{A}^{j}$ is a component of an axial vector quantity like a spin or an angular momentum operator. The real coefficients $C_{\{n\}}$ carry a multi-index $\{n\}$, which includes summations inherent to the method of the evaluation of the E_{pv}. Such a multi-index could contain indices of molecular orbitals, of atomic centers, of atomic basis functions, and of CIS-excited states as it is in the present paper or, in the more complicated case of using unrestricted molecular orbitals, it could include spin-orbital indices. Using such a representation, one writes the total E_{pv} as a trace of this tensor:

$$E_{\mathrm{pv}}=\mathrm{Tr}\ E_{\mathrm{pv}}^{i,j}=E_{\mathrm{pv}}^{xx}+E_{\mathrm{pv}}^{yy}+E_{\mathrm{pv}}^{zz}. \tag{5}$$

Thus such a tensor transforms under the Cartesian coordinate transformations as a polar vector in its first index and as an axial vector in its second index. It is seen that the $E_{\mathrm{pv}}^{i,j}$ tensor has as its trace a pseudoscalar which is required for detection of parity asymmetry.

To obtain more reliable numerical values of E_{pv} we develop a new formalism for the evaluation of E_{pv}, rejecting the restriction to *single-determinant* excited states produced from RHF wave function by means of substitution of one molecular orbital. Instead, we study the effect of using flexible linear combinations of such determinants, CIS wave functions, on the value of E_{pv} and on its dependence upon the geometry of molecules. Since the overall wave function obtained is now a perturbation-theory admixture of the ground RHF state with the CIS excited states, we shall call it CIS-RHF formalism. Such an approach has two advantages: it uses improved quality wave functions and improved energy denominators for the perturbation theory with spin-orbit interaction. As we shall see, this new approach in some instances leads to a change of the order of magnitude of E_{pv} as compared to previous SDE-RHF calculations. A preliminary account of our results with the new CIS-RHF method has been given in Ref. 48.

II. THEORY OF PARITY VIOLATING ENERGIES IN MOLECULES

A. Effective form of the parity violating interaction

To derive the effective form of the electron–neutron parity violating interaction in molecules, let us first consider the pairwise electron–neutron weak interaction.[49,50] According to the standard model of the electroweak interactions,[4–6] this interaction is mediated by the electrically neutral Z^0 bosons. However, at the energies which are appreciably less than the rest mass of the Z^0 boson, i.e., less than $91.19\ \mathrm{GeV}/c^2$, the contribution of the Z^0 bosons becomes virtual.[51] The interaction acquires the form of the (vector current) $\times$(axial current) product (see also Refs. 52 and 53, as well as Refs. 54–57, where the effect of parity violation on optical rotation in atoms and diatomic molecules has been reviewed). The first quantity entering such an interaction is the 4-vector current.[58] Here we use the relativistic system of units: $\hbar=c=1$. Let $j^{\mu}[\psi^{(\mathrm{n})}(x)]$ and $j^{\nu}[\psi^{(\mathrm{el})}(x)]$ be the 4-vector currents formed from the wave functions of neutron $\psi^{(\mathrm{n})}(x)$ and electron $\psi^{(\mathrm{el})}(x)$, respectively. Since these wave functions are the four-components operator bispinors, taken in the representation of second quantization,[58] the 4-vector relativistic current is defined by means of the use of the familiar γ matrices:[58]

$$j^{\mu}[\psi(x)]\overset{\mathrm{def}}{=}:\psi^{\dagger}(x)\gamma^{0}\gamma^{\mu}\psi(x):, \tag{6}$$

where the colon represents the normal ordering of the operators entering this expression, i.e., all annihilation operators appear to the right from the creation operators,[58] eliminating therefore nonphysical nonzero expectation values at the vacuum state. Furthermore, $\psi^{\dagger}(x)$ is a 4-component operator bispinor, which is conjugate to $\psi(x)$.

The other quantities of importance are the relativistic axial currents[58] of neutrons and electrons, $j^{\mu}_{(\mathrm{ax})}[\psi^{(\mathrm{n})}(x)]$ and $j^{\nu}_{(\mathrm{ax})}[\psi^{(\mathrm{el})}(x)]$, respectively. The axial currents obey the following definition, which differs from (6) by the presence of the additional γ^5 matrix:[58]

$$j^{\mu}_{(\mathrm{ax})}[\psi(x)]\overset{\mathrm{def}}{=}:\psi^{\dagger}(x)\gamma^{0}\gamma^{\mu}\gamma^{5}\psi(x):. \tag{7}$$

The presence of the γ^5 matrix is important, it converts the 4-vector $j^{\mu}[\psi(x)]$ into the axial vector $j^{\mu}_{(\mathrm{ax})}[\psi(x)]$. Thus at low energies the relativistic Hamiltonian density of the parity violating part of the weak electron–neutron interaction becomes a product of these two currents multiplied by the proper constants:[49–51]

$$\hat{\mathscr{H}}^{(\mathrm{e-n})}(x)=\frac{G_{\mathrm{F}}}{2\sqrt{2}}\,g_{\mathrm{A}}(1-4\sin^2\Theta_{\mathrm{W}})j_{\mu}[\psi^{(\mathrm{el})}(x)]\times j^{\mu}_{(\mathrm{ax})}[\psi^{(\mathrm{n})}(x)]+\frac{G_{\mathrm{F}}}{2\sqrt{2}}\,j_{\mu}[\psi^{(\mathrm{n})}(x)]\times j^{\mu}_{(\mathrm{ax})}[\psi^{(\mathrm{el})}(x)]. \tag{8}$$

Here the relativistic summation over repeated indices is assumed,[51] with the relativistic scalar product of two 4-vectors $a=(a_0,\mathbf{a})$ and $b=(b_0,\mathbf{b})$ defined as $a_{\mu}b^{\mu}=a_0b_0$

$-\mathbf{ab}$. G_F is the Fermi constant,[49,50,59,60] which can be scaled by the mass of the proton M_p as $G_F M_p^2 \approx 1.027 \times 10^{-5}$. The form-factor g_A originates from the strong interaction of the neutron and could be taken as equal to 1.25.[49,50] The current experimental value of the Weinberg parameter $\sin^2 \Theta_W$ is 0.2319(5).[59,60] At this value of Θ_W the factor $(1-4 \sin^2 \Theta_W)$ is small (≈ 0.08).

In the (current)×(axial current) representation the electron–proton parity violating interaction has a form similar to (8):

$$\hat{\mathscr{H}}^{(e-p)}(x) = -\frac{G_F}{2\sqrt{2}} g_A (1-4 \sin^2 \Theta_W) j_\mu[\psi^{(el)}(x)] j^\mu_{(ax)}[\psi^{(p)}(x)] - \frac{G_F}{2\sqrt{2}} (1-4 \sin^2 \Theta_W) j_\mu[\psi^{(p)}(x)] j^\mu_{(ax)}[\psi^{(el)}(x)]. \quad (9)$$

The relativistic electron–electron parity violating interaction has the form:

$$\hat{\mathscr{H}}^{(e-e)}(x) = \frac{G_F}{\sqrt{2}} (1-4 \sin^2 \theta_W) j_\mu[\psi^{(el)}(x)] j^\mu_{(ax)}[\psi^{(el)}(x)]. \quad (10)$$

Note that the expression (10) possesses no factor of 1/2 which is compensated for due to the exchange interaction.[49,61] The technique of calculation (Fierz reshuffle) is explained, for instance, in Ref. 58. Thus this correct expression and its nonrelativistic form differ by a factor of 2 from the expressions presented in some previous work.[12,62]

Atomic and molecular energies are many orders of magnitude less than the rest energy of the electron (≈ 0.5 MeV), thus the nonrelativistic approximation must be good at least for $Z<50$, as has been discussed in detail in Refs. 49, 62, and 63. Furthermore, the averaged velocity of neutrons in nuclei is much less than the velocity of electrons: so, the approximation of small neutron velocities[64,65] is applied when all quantities, which are proportional to the ratio of the neutron momentum to neutron mass, $\mathbf{P}_n/M_n$, are neglected.

Performing the nonrelativistic approximation, i.e., omitting two ''small'' components of bispinors $\psi^{(n)}(x)$ and $\psi^{(el)}(x)$ and therefore converting the formulation of the theory from four-component bispinors to two-component spinors, changing correspondingly from the relativistic system of units to atomic units, and performing small neutron velocity approximation, one arrives at the Hamiltonian density:[62,63]

$$\hat{\mathscr{H}}^{(e-n)}(\mathbf{x}) = \frac{G_F}{4\sqrt{2}\mu c} [-\psi^{\dagger(n)}(\mathbf{x})\psi^{(n)}(\mathbf{x})\{\psi^{\dagger(el)}(\mathbf{x})\boldsymbol{\sigma}(\mathbf{P}\psi^{(el)}(\mathbf{x})) + (\mathbf{P}^*\psi^{\dagger(el)}(\mathbf{x}))\boldsymbol{\sigma}\psi^{(el)}(\mathbf{x})\} + i g_A (1-4 \sin^2 \Theta_W) \times \mathbf{P}(\psi^{\dagger(el)}(\mathbf{x})\boldsymbol{\sigma}\psi^{(el)}(\mathbf{x}))\psi^{\dagger(n)}(x)\boldsymbol{\sigma}\psi^{(n)}(\mathbf{x})]. \quad (11)$$

$\mathbf{P}$ is the momentum operator, $\boldsymbol{\sigma}$ is the doubled spin operator which has as its components the familiar 2×2 Pauli matrices, $\mathbf{x}$ is the set of spatial coordinates, μ is the reduced electron mass, and c is the speed of light *in vacuo*. The last term in this expression is believed[62–65] to be small compared to the first one for two reasons: (i) it has as a factor $(1-4 \sin^2 \Theta_W) \approx 0.08$ and (ii) it depends on the neutron spin while, in their low-energy states, the atomic nuclei have a tendency to possess mutually compensated spins of hadrons. Thus the second term in Eq. (11) is usually dropped. Furthermore, on an atomic scale of distances (10^{-10} m) one can replace the neutron density, to a very good approximation, by the δ function (really about 10^{-15} m):

$$\psi^{\dagger(n)}(\mathbf{x})\psi^{(n)}(\mathbf{x}) \approx \delta^3(\mathbf{x}-\mathbf{x}^{(n)}), \quad (12)$$

where $\mathbf{x}^{(n)}$ is the neutron spatial position. The Hamiltonian density (11) and (12) corresponds to the following one-electron Hamiltonian operator:[62,63]

$$\hat{H}^{(e-n)} = -\frac{G_F}{4\sqrt{2}\mu c} (\mathbf{P}\boldsymbol{\sigma}\delta^3(\mathbf{x}-\mathbf{x}^{(n)}) + \delta^3(\mathbf{x}-\mathbf{x}^{(n)})\mathbf{P}\boldsymbol{\sigma}). \quad (13)$$

Repeating the same transformations with respect to the electron–proton parity violating interaction (9) one finds the corresponding form of it which is effective for atoms and molecules:

$$\hat{H}^{(e-p)} = \frac{G_F}{4\sqrt{2}\mu c} (1-4 \sin^2 \Theta_W) \times (\mathbf{P}\boldsymbol{\sigma}\delta^3(\mathbf{x}-\mathbf{x}^{(p)}) + \delta^3(\mathbf{x}-\mathbf{x}^{(p)})\mathbf{P}\boldsymbol{\sigma}). \quad (14)$$

Apparently, the electron–neutron parity violating interaction is the leading one[62–65] while the electron–proton interaction is about one order of magnitude smaller. It is convenient to combine the operators (13) and (14) together, denoting the radius-vector to the nucleus as $\mathbf{x}^{nucl}$ and noticing that $\mathbf{x}^n = \mathbf{x}^p = \mathbf{x}^{nucl}$ in the approximation of the pointlike nucleus. Thus one obtains the effective electron–nucleus parity violating interaction by means of summation over all the hadrons in the nucleus:

$$\hat{H}^{(e-nucl)} = \frac{G_F}{4\sqrt{2}\mu c} Q^c_W(A) \times (\mathbf{P}\boldsymbol{\sigma}\delta^3(\mathbf{x}-\mathbf{x}^{nucl}) + \delta^3(\mathbf{x}-\mathbf{x}^{nucl})\mathbf{P}\boldsymbol{\sigma}). \quad (15)$$

Here $Q^c_W(A)$ is the electroweak charge of the nucleus A, expressed through the number of protons Z, number of neutrons N, and the Weinberg angle Θ_W:

$$Q^c_W(A) = Z(1-4 \sin^2 \Theta_W) - N. \quad (16)$$

Thus the electroweak charge results from the summation of the one-electron operators $\hat{H}^{(e\text{-}n)}$ and $\hat{H}^{(e\text{-}p)}$ in (13) and (14) over the N neutrons and Z protons present in the nucleus.

The existing estimates[49] for the contribution of the electron–electron parity violating interaction (10) indicate that it should not exceed 1% of the sum of contributions of the electron–hadron parity violating interactions. In the nonrelativistic approximation, the electron–electron parity violating interaction acquires the form:[62]

$$\hat{\mathscr{H}}^{(\mathrm{e-e})} = -\frac{G_F}{2\sqrt{2}\mu c}(1-4\sin^2\theta_W) \times (\{\delta^3(\mathbf{x}^{(1)}-\mathbf{x}^{(2)}),(\boldsymbol{\sigma}^{(1)}-\boldsymbol{\sigma}^{(2)})\cdot(\mathbf{P}^{(1)}-\mathbf{P}^{(2)})\}_+ + i[\delta^3(\mathbf{x}^{(1)}-\mathbf{x}^{(2)}),(\boldsymbol{\sigma}^{(1)}\times\boldsymbol{\sigma}^{(2)})\cdot(\mathbf{P}^{(1)}-\mathbf{P}^{(2)})]). \quad (17)$$

Here $\{\ldots,\ldots\}_+$ denotes an anticommutator while [...,...] is a commutator.

B. Perturbation by the spin-orbit interaction

Given a molecular wave function $|\Psi_{\mathrm{mol}}\rangle$, the mean value E_{pv} of the parity violating interaction is naturally defined as

$$E_{\mathrm{pv}} = \langle\Psi_{\mathrm{mol}}|\hat{H}_{\mathrm{pv}}|\Psi_{\mathrm{mol}}\rangle, \quad (18)$$

where one assumes in place of $\hat{H}_{\mathrm{pv}}$ one of the operators (13), (14), or (17), or in practice the sum in Eq. (15). Elementary molecular orbital theory[66,67] includes for the evaluation of the molecular wave function $|\Psi_{\mathrm{mol}}\rangle$ only the Coulomb interaction between the constituents of molecules, nuclei and electrons, while the parity violating interactions (13), (14), or (17) are entangled mostly with the magnetic properties of molecules due to their essential dependence on spin. Thus the wave function which has no full account for the magnetic properties of a molecule is likely to be insensitive to the parity violating properties. In order to illustrate this, one can partition the molecular wave function $|\Psi_{\mathrm{mol}}\rangle$ into a part due to Coulomb interaction $|\Psi_{\mathrm{Coul}}\rangle$ and a part due to magnetic interactions $|\Psi_{\mathrm{magn}}\rangle$

$$|\Psi_{\mathrm{mol}}\rangle = |\Psi_{\mathrm{Coul}}\rangle + |\Psi_{\mathrm{magn}}\rangle, \quad (19)$$

$$E_{\mathrm{pv}} = \langle\Psi_{\mathrm{Coul}}|\hat{H}_{\mathrm{pv}}|\Psi_{\mathrm{Coul}}\rangle + 2\,\mathrm{Re}\langle\Psi_{\mathrm{Coul}}|\hat{H}_{\mathrm{pv}}|\Psi_{\mathrm{magn}}\rangle + \langle\Psi_{\mathrm{magn}}|\hat{H}_{\mathrm{pv}}|\Psi_{\mathrm{magn}}\rangle. \quad (20)$$

Regardless of the method of the evaluation of $|\Psi_{\mathrm{Coul}}\rangle$, the elementary techniques do not take into account magnetic properties and thus the resulting molecular wave function is just the Coulombic part of the desired full wave function of the molecule:

$$|\Psi_{\mathrm{mol}}^{\mathrm{stand}}\rangle = |\Psi_{\mathrm{Coul}}\rangle. \quad (21)$$

In the framework of the RHF evaluation, when $|\Psi_{\mathrm{mol}}^{\mathrm{stand}}\rangle = |\Psi_{\mathrm{RHF}}\rangle$, the spin components of the spin-orbitals are identical. This leads to zero expectation value of the operators $\hat{H}^{(\mathrm{e\text{-}n})}$ and $\hat{H}^{(\mathrm{e\text{-}p})}$ in (13) and (14) with respect to such a molecular wave function:

$$E_{\mathrm{pv}} = \langle\Psi_{\mathrm{RHF}}|\hat{H}_{\mathrm{pv}}|\Psi_{\mathrm{RHF}}\rangle \equiv 0. \quad (22)$$

This can be easily verified by a straightforward analytical calculation of matrix elements of the operators (13) and (14) for the RHF molecular wave function.[12]

There are at least two possible ways for generating the indispensible magnetic wave function $|\Psi_{\mathrm{magn}}\rangle$. One way of doing this is obviously to include the magnetic interaction terms $\hat{H}_{\mathrm{magn}}$ both into the initial self-consistent field (SCF) calculation and into post-SCF calculations, expanding therefore the fundamental Hamiltonian $\hat{H}^{(\mathrm{MO})}$, used by the MO theory, beyond the simplistic Coulomb interaction $\hat{H}_{\mathrm{Coul}}$:

$$\hat{H}^{(\mathrm{MO})} = \hat{H}_{\mathrm{Coul}}; \Rightarrow \hat{H}^{(\mathrm{MO})} = \hat{H}_{\mathrm{Coul}} + \hat{H}_{\mathrm{magn}}. \quad (23)$$

The theoretical ground work, accounting for leading magnetic terms, is sufficiently developed,[68–71] and ab initio calculations for spin-orbit interaction and accompanying effects have also been done.[70,72] We plan work along these lines for ΔE_{pv}. However, at present, we have chosen another obvious way for the calculation of the magnetic effects by the use of perturbation theory. To get nonzero values of the operators $\hat{H}^{(\mathrm{e\text{-}n})}$ and $\hat{H}^{(\mathrm{e\text{-}p})}$ one can consider a perturbation of the RHF molecular wave function by an interaction which affects its spin properties and mixes the RHF ground state with the nearest excitations. The strongest interaction of this kind is, normally, the spin-orbit interaction.[66,73,74] In the approximation of the spherical Coulomb field of the nucleus, the expression for the spin–orbit interaction of electrons and nucleus is written as:[73]

$$\hat{H}^{(\mathrm{so})} = \frac{\alpha^2}{4}\sum_i f(r_i)\boldsymbol{\sigma}_i\mathbf{L}_i, \quad (24)$$

where $\mathbf{L}_i$ is the angular momentum operator of the ith electron in the atom, $f(r_i)$ is the effective, distance-dependent spin-orbit coupling for the same electron. The operators of electron–hadron parity violating interactions (13)–(15) and of the spin-orbit interaction (24) are all additive one-electron quantities.

The perturbation of the ground state $|\Psi_0\rangle$ of a molecule due to the spin-orbit interaction can be written as follows:

$$|\Psi_0\rangle \rightarrow |\tilde{\Psi}_0\rangle = |\Psi_0\rangle + \sum_n \frac{\langle\Psi_n|\hat{H}^{(\mathrm{so})}|\Psi_0\rangle}{E_0-E_n}|\Psi_n\rangle, \quad (25)$$

where $|\Psi_n\rangle$ is assumed to be the nth excited state and E_n its energy, while E_0 is the energy of the ground state $|\Psi_0\rangle$. The leading contribution to the mean value E_{pv} of the electron–nucleus parity violating weak interaction $\hat{H}^{(\mathrm{e\text{-}nucl})}$ over such a wave function is

$$E_{\mathrm{pv}} = 2\,\mathrm{Re}\left\{\sum_n \frac{\langle\Psi_0|\hat{H}^{(\mathrm{e-nucl})}|\Psi_n\rangle\langle\Psi_n|\hat{H}^{(\mathrm{so})}|\Psi_0\rangle}{E_0-E_n}\right\}. \quad (26)$$

C. Parity violating interaction in the SDE-RHF framework

One can take advantage of knowing the structure of the RHF molecular wave function, restricting attention to single-determinant excitations only (SDE). Since the RHF wave function is a single determinant,[66] formed from spin-orbitals with identical α and β spin components,[66] and since only those single excitations are contributing to (26) which create triplet excitations,[12] one can easily factorize out the spin operator dependence,[12] perform the summation over the identical electrons, and rewrite the mean value (26) in terms of only one-electron operators and spatial molecular orbitals of the ground single-determinant state and singly excited determinants.[12,16,19] In addition, approximating the energy denominators by the difference between corresponding mo-

lecular orbital energies (for an attempt to improve upon this approximation, see Ref. 19), one obtains the expression which has been used for the evaluation of the parity violating energies in molecules in practically all contemporary work[12–32] for $E_{\rm pv}$:

$$E_{\rm pv}=\frac{\alpha G_{\rm F}}{\sqrt{2}}\sum_{I\in {\rm occ.}}\sum_{J\in {\rm virt.}}\frac{1}{\epsilon_I-\epsilon_J}\langle\Psi_I|\hat{\mathscr{P}}|\Psi_J\rangle\langle\Psi_J|\hat{\Lambda}|\Psi_I\rangle, \tag{27}$$

$$\{\Psi\}:\ {\rm Im}|\Psi_I\rangle\equiv{\rm Im}|\Psi_J\rangle\equiv 0. \tag{28}$$

Here $G_{\rm F}$ is, as before, the Fermi constant, α is the fine structure constant, $|\Psi_I\rangle$ and $|\Psi_J\rangle$ are the Ith occupied molecular orbital and the Jth virtual molecular orbital of the molecule under consideration, and ϵ_I and ϵ_J are corresponding molecular orbital energies.

Further, the $\hat{\mathscr{P}}$ operator is proportional to the anticommutator of the operator of the momentum of an electron in molecule with a three-dimensional δ function centered on nucleus A:

$$\hat{\mathscr{P}}=\sum_A Q_{\rm W}^c(A)\sum_{k=1}^{3}\{\hat{P}_k,\delta^3(\mathbf{r}-\mathbf{r}_A)\}_+\mathbf{e}_k;$$

$$\text{with}\quad \hat{P}_k=-i\frac{\partial}{\partial x_k}, \tag{29}$$

where A is the index of an atomic center, $\mathbf{e}_k$ is the unit vector in the direction k so that $\mathbf{r}=\Sigma_k x_k\mathbf{e}_k$, and the coefficient $Q_{\rm W}^c(A)$ is the effective electroweak charge[50] of an atom A defined in (16).

The $\hat{\Lambda}$ operator is the orbital angular momentum part of the operator of spin-orbit coupling of electrons (see previous section):

$$\hat{\Lambda}=\sum_B\sum_{m=1}^{3}\hat{\Lambda}_{B,m}\mathbf{e}_m,\quad \hat{\Lambda}_{B,m}=-\frac{\alpha^2}{4}\frac{1}{r}\frac{\partial U_B}{\partial r}\hat{L}_m, \tag{30}$$

where U_B is electrostatic potential energy of an electron in the spherical self-consistent field of the Bth atomic center, r is the modulus of the radius-vector for the electron and $\hat{L}_m$ is the mth component of the orbital angular momentum operator of the electron. The coefficient $\alpha^2/4$ is twice less than the customarily used form[66] and corresponds to the direct use of Pauli matrices as in the work by Hegstrom *et al.*[12] In Refs. 13–30 spin 1/2 operators were used instead.

Following Ref. 48, we substitute (29) and (30) into (27) and get both the tensor components $E_{\rm pv}^{i,j}$ and the total $E_{\rm pv}$, as it was defined in (4) and (5):

$$E_{\rm pv}^{i,j}=\frac{\alpha G_{\rm F}}{\sqrt{2}}\sum_A Q_{\rm W}^c(A)\sum_{I\in {\rm occ.}}\sum_{J\in {\rm virt.}}\sum_B\frac{1}{\epsilon_I-\epsilon_J}$$
$$\times\langle\Psi_I|\{\hat{P}_i,\delta^3(\mathbf{r}-\mathbf{r}_A)\}_+|\Psi_J\rangle\langle\Psi_J|\hat{\Lambda}_{B,j}|\Psi_I\rangle, \tag{31}$$

$$E_{\rm pv}={\rm Tr}\,E_{\rm pv}^{i,j}=E_{\rm pv}^{xx}+E_{\rm pv}^{yy}+E_{\rm pv}^{zz}, \tag{32}$$

$$E_{\rm pv}=\frac{\alpha G_F}{\sqrt{2}}\sum_A Q_W^c(A)\sum_{I\in {\rm occ.}}\sum_{J\in {\rm virt.}}\sum_B\sum_{k=1}^{3}\frac{1}{\epsilon_I-\epsilon_J}$$
$$\times\langle\Psi_I|\{\hat{P}_k,\delta^3(\mathbf{r}-\mathbf{r}_A)\}_+|\Psi_J\rangle\langle\Psi_J|\hat{\Lambda}_{B,k}|\Psi_I\rangle. \tag{33}$$

If one employes the conventional LCAO method.[66,67] and writes the molecular orbitals $|\Psi_I\rangle$ and $|\Psi_J\rangle$ as linear combination of the real atomic orbitals centered on nuclei A and B: (We represent the index of the atomic orbital as a set of two indices: index of the atomic center A and index of the atomic orbital centered at this particular center, $\mu(A)$. One will see that this representation allows us later to easier state an additional, single-center, approximation which is used on top of approximations stated before.)

$$|\Psi_I\rangle=\sum_A\sum_{\mu(A)}C(I,A,\mu(A))|\phi(A,\mu(A))\rangle, \tag{34}$$

$$|\Psi_J\rangle=\sum_B\sum_{\nu(B)}C(J,B,\nu(B))|\phi(B,\nu(B))\rangle, \tag{35}$$

$${\rm Im}|\phi(A,\mu(A))\rangle\equiv 0,\forall\{A,\mu(A)\}, \tag{36}$$

then one discovers that the expression (33) is, in fact, even more cumbersome than it looks, for the matrix elements entering into it are still other sums:

$$\langle\Psi_I|\{\hat{P}_k,\delta^3(\mathbf{r}-\mathbf{r}_A)\}_+|\Psi_J\rangle$$
$$=\sum_{A'}\sum_{\mu'(A')}\sum_{B'}\sum_{\nu'(B')}C(I,A',\mu'(A'))$$
$$\times C(J,B',\nu'(B'))$$
$$\times\langle\phi(A',\mu'(A'))|\{\hat{P}_k,\delta^3(\mathbf{r}_A)\}_+|\phi(B',\nu'(B'))\rangle, \tag{37}$$

$$\langle\Psi_J|\hat{\Lambda}_{B,k}|\Psi_I\rangle$$
$$=\sum_{A''}\sum_{\mu''(A'')}\sum_{B''}\sum_{\nu''(B'')}C(J,B'',\nu''(B''))$$
$$\times C(I,A'',\mu''(A''))$$
$$\times\langle\phi(B'',\nu''(B''))|\hat{\Lambda}_{B,k}|\phi(A'',\mu''(A''))\rangle. \tag{38}$$

As the atomic orbitals are taken to be real[66,67] one can rewrite Eqs. (37) and (38), with the explicit factor i:[12,16]

$$\langle\Psi_I|\{\hat{P}_k,\delta^3(\mathbf{r}-\mathbf{r}_A)\}_+|\Psi_J\rangle$$
$$=i\sum_{A'}\sum_{\mu'(A')}\sum_{B'}\sum_{\nu'(B')}C(I,A',\mu'(A'))$$
$$\times C(J,B',\nu'(B'))$$
$$\times P(A,k|A',\mu'(A'),B',\nu'(B')), \tag{39}$$

$$\langle\Psi_J|\hat{\Lambda}_{B,k}|\Psi_I\rangle$$
$$=i\sum_{A''}\sum_{\mu''(A'')}\sum_{B''}\sum_{\nu''(B'')}C(J,B'',\nu''(B''))$$
$$\times C(I,A'',\mu''(A''))$$
$$\times\Lambda(B,k|B'',\nu''(B''),A'',\mu''(A'')), \tag{40}$$

where the quantities $P(A,k|A',\mu'(A'),B',\nu'(B'))$ and $\Lambda(B,k|B'',\nu''(B''),A'',\mu''(A''))$ are now strictly real and correspond to the matrix elements on the right-hand sides of (37) and (38). One gets their explicit forms comparing (39) and (40) with (37) and (38) and the definitions (29) and (30).

Combining (33), (39), and (40), one obtains:

$$E_{\mathrm{pv}}=-\frac{\alpha G_{\mathrm{F}}}{\sqrt{2}}\sum_{A}Q_{\mathrm{W}}^{c}(A)\sum_{I\in\mathrm{occ.}}\sum_{J\in\mathrm{virt.}}\frac{1}{\epsilon_I-\epsilon_J}\sum_{B}\sum_{k=1}^{3}\sum_{A'}\sum_{\mu'(A')}\sum_{B'}\sum_{\nu'(B')}C(I,A',\mu'(A'))C(J,B',\nu'(B'))$$
$$\times\sum_{A''}\sum_{\mu''(A'')}\sum_{B''}\sum_{\nu''(B'')}C(I,A'',\mu''(A''))C(J,B'',\nu''(B''))P(A,k|A',\mu'(A'),B',\nu'(B'))$$
$$\times\Lambda(B,k|B'',\nu''(B''),A'',\mu''(A'')). \tag{41}$$

Apart from MO coefficients and MO energies, the main quantities of interest are the matrix elements $P(A,k|A',\mu'(A'),B',\nu'(B'))$ and $\Lambda(B,k|B'',\nu''(B''),A'',\mu''(A''))$.

The distinctive feature of these matrix elements is that they are, in general, rather unusual three-center quantities. Indeed, the matrix element $\Lambda(B,k|B'',\nu''(B''),A'',\mu''(A''))$ has two, generally different centers at which the atomic orbitals are defined and, in addition, the third center at which the electrostatic potential defining the spin-orbit coupling is centered. Similarly, the matrix element $P(A,k|A',\mu'(A'),B',\nu'(B'))$ has two centers for atomic orbitals and the third center at which the three-dimensional δ-function is centered. An attempt to evaluate these matrix elements, as they are standing in (41), especially the one for spin-orbit coupling, would lead to appreciable technical complications even in the framework of the Gaussian representation of atomic orbitals.

However, both matrix elements seem to be[12] heavily weighted towards regions containing the center of the electrostatic potential or the center for the δ-function. It is therefore likely that the overlap, defined by vanishingly small values at the tails of atomic orbitals, can be neglected and the matrix elements can be restricted to the single center. So, the single-center approximation may be formulated by the relations

$$P(A,k|A',\mu'(A'),B',\nu'(B'))$$
$$\approx P(A,k|\mu'(A),\nu'(A))\,\delta_{A,A'}\,\delta_{A,B'}, \tag{42}$$

$$\Lambda(B,k|B'',\nu''(B''),A'',\mu''(A''))$$
$$\approx\Lambda(B,k|\nu''(B),\mu''(B))\,\delta_{B,A''}\delta_{B,B''}. \tag{43}$$

The explicit form of the matrix elements $P(A,k|\mu'(A),\nu'(A))$ and $\Lambda(B,k|\nu''(B),\mu''(B))$ will be specified below, together with the specification of the s and p basis functions, which are the only basis functions giving nonzero values for these matrix elements.

With the single-center approximation for matrix elements (neglect for overlap effects), the E_{pv} expression (41) simplifies finally into:

$$E_{\mathrm{pv}}=-\frac{\alpha G_{\mathrm{F}}}{\sqrt{2}}\sum_{A}Q_{\mathrm{W}}^{c}(A)\sum_{I\in\mathrm{occ.}}\sum_{J\in\mathrm{virt.}}\frac{1}{\epsilon_I-\epsilon_J}$$
$$\times\sum_{B}\sum_{k=1}^{3}\sum_{\mu'(A)}\sum_{\nu'(A)}C(I,A,\mu'(A))C(J,A,\nu'(A))$$
$$\times\sum_{\mu''(B)}\sum_{\nu''(B)}C(I,B,\mu''(B))C(J,B,\nu''(B))$$
$$\times P(A,k|\mu'(A),\nu'(A))\Lambda(B,k|\nu''(B),\mu''(B)). \tag{44}$$

Since the matrix elements are now confined to single centers, we can present them in somewhat more concise form. Let the atomic orbitals $|\phi(A,\mu(A))\rangle$ in (34) and (35) be factorized into their radial $|R(A,\mu(A))\rangle$ and angular $|Y(A,\mu(A))\rangle$ parts:

$$|\phi(A,\mu(A))\rangle=|R(A,\mu(A))\rangle\otimes|Y(A,\mu(A))\rangle. \tag{45}$$

Then the matrix element $P(A,k|\mu'(A),\nu'(A))$ will be different from zero only between $n's$ and $n''p$ atomic orbitals, whichever orbitals are used in the atomic basis set (One has to differentiate the δ-function too, using: $\int\delta'(x)F(x)dx=-F'(0)$.):

$$P(A,k|n's,n''p_q)=-P(A,k|n''p_q,n's)$$
$$=-\frac{\sqrt{3}}{4\pi}\,\delta_{kq}\left(R(n's)\,\frac{dR(n''p_q)}{dr}\right)_{r=r_A}. \tag{46}$$

It is assumed that the p functions are Cartesian, i.e., vector indices k and q refer to Cartesian axes. The imaginary unit has been already factorized out in (39) and (40) and does not enter here.

The matrix element $\Lambda(B,k|\nu''(B),\mu''(B))$ is equal to the following product:

$$\Lambda(B,k|\nu(B),\mu(B))$$
$$=-\frac{\alpha^2}{4}\left\langle R(B,\nu(B))\left|\frac{1}{r}\frac{\partial U_B}{\partial r}\right|R(B,\mu(B))\right\rangle$$
$$\times\langle Y(B,\nu(B))|\hat{L}_k|Y(B,\mu(B))\rangle. \tag{47}$$

The angular momentum matrix element $\langle Y(B,\nu(B))|\hat{L}_k|Y(B,\mu(B))\rangle$ shows that (47) is different from zero for states with nonzero angular momentum: *p*, *d*, and so on. When the matrix element (47) is diagonal with respect to subshells, i.e., when it is taken between two *p* states or two *d* states or two *f* states, it can be expressed[12] through the conventional single-electron spin-orbit coupling parameters[73] which helps to introduce into the calculations experimental quantities known from atomic spectroscopy.[12]

D. CIS-RHF approach to evaluations of E_{pv}

The SDE-RHF formalism needs appreciable improvement, which might be possible with more sophisticated calculations of the molecular wave function using, for instance, the Møller–Plesset (MP) perturbation theory and configuration interaction (CI) theory. The main deficiency of the SDE-RHF wave function is connected, generally, with the unsatisfactory quality of SDE states. So, one must first attempt a better representation of the excited states.

To develop the formalism which allows one to evaluate the E_{pv} values taking into account the CIS method for the excited states[75] one has to again start with the relation (26):

$$E_{pv}=2\,\mathrm{Re}\left\{\sum_n \frac{\langle\Psi_0|\hat{H}^{(e-n)}|\Psi_n\rangle\langle\Psi_n|\hat{H}^{(so)}|\Psi_0\rangle}{E_0-E_n}\right\}. \quad (48)$$

In contrast to the stiff single determinant excitations, the excited states $|\Psi_n\rangle$ are now defined as the flexible linear combinations of independent Slater determinants. These linear combinations are obtained by means of the single substitution of the new spin orbital with index *j* into the reference RHF determinant $|D_0\rangle$ instead of the spin orbital with index *i*. We denote such a new determinant as $|D_i^j\rangle$ and write down the linear combinations of them which are entering the CIS as

$$|\Psi_n\rangle=\sum_i\sum_j a_i^j(n)|D_i^j\rangle. \quad (49)$$

The basis determinants $\{|D_i^j\rangle\}$ for all excited states are the same, their relative contribution into excited state $|\Psi_n\rangle$ being determined through the set of coefficients $\{a_i^j(n)\}$.

The expression (48) is now to be rewritten as

$$E_{pv}=\sum_n \frac{1}{E_0-E_n}\sum_i\sum_j\sum_k\sum_l a_i^j(n)a_k^l(n)\times\{\langle D_0|\hat{H}^{(e-n)}|D_i^j\rangle\langle D_k^l|\hat{H}^{(so)}|D_0\rangle + \text{complex conjugate}\}. \quad (50)$$

Denoting now the spin orbitals as $|\tilde{\Psi}_i\rangle$ we recall the well-known relations for the matrix elements of one-electron operators with respect to determinantal wave function obtained by means of single substitutions. For the case under consideration they are

$$\langle D_0|\hat{H}^{(e-n)}|D_i^j\rangle\equiv\langle\tilde{\Psi}_i|\hat{H}^{(e-n)}|\tilde{\Psi}_j\rangle, \quad (51)$$

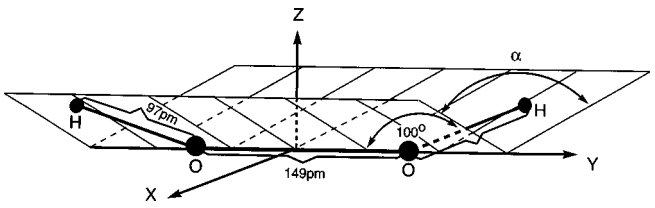

FIG. 2. The standard orientation, employed in our CIS-RHF calculations of E_{pv}, is shown for an H_2O_2 molecule. At this orientation, the selection rules for the perturbation theory contributions to E_{pv} with respect to *A*-symmetric ground state are as follows: *A*-symmetric excited states contribute only to E_{pv}^{zz} while *B*-symmetric excited states contribute to both E_{pv}^{xx} and E_{pv}^{yy}. This selection rule is determined by the fact that the only symmetry element, C_2 rotation by angle π about *Z* axis, leaves the *Z* axis unchanged while reversing the direction of *X* and *Y* axes.

$$\langle D_k^l|\hat{H}^{(so)}|D_0\rangle\equiv\langle\tilde{\Psi}_l|\hat{H}^{(so)}|\tilde{\Psi}_k\rangle. \quad (52)$$

Substituting this into (50), we have

$$E_{pv}=\sum_n \frac{1}{E_0-E_n}\sum_i\sum_j\sum_k\sum_l a_i^j(n)a_k^l(n)\times\{\langle\tilde{\Psi}_i|\hat{H}^{(e-n)}|\tilde{\Psi}_j\rangle\langle\tilde{\Psi}_l|\hat{H}^{(so)}|\tilde{\Psi}_k\rangle + \text{complex conjugate}\}. \quad (53)$$

After performing the summation over the spin variables,[16,17] one rewrites this expression in terms of the molecular orbitals $|\Psi_I\rangle$ instead of spin orbitals $|\tilde{\Psi}_i\rangle$, and in terms of the operators $\hat{\mathscr{P}}$ and $\hat{\Lambda}$ which are defined in (29) and (30), respectively, instead of the operators $\hat{H}^{(e-n)}$ and $\hat{H}^{(so)}$:

$$E_{pv}=\frac{\alpha G_F}{\sqrt{2}}\sum_n \frac{1}{E_0-E_n}\sum_I\sum_J\sum_K\sum_L a_I^J(n)a_K^L(n)\times\langle\Psi_I|\hat{\mathscr{P}}|\Psi_J\rangle\langle\Psi_L|\hat{\Lambda}|\Psi_K\rangle. \quad (54)$$

Employing the explicit expressions (29) and (30) for the operators $\hat{\mathscr{P}}$ and $\hat{\Lambda}$, one obtains:

$$E_{pv}=\frac{\alpha G_F}{\sqrt{2}}\sum_n \frac{1}{E_0-E_n}\sum_A Q_W^c(A)\sum_I\sum_J\sum_K\sum_L \times a_I^J(n)a_K^L(n)\sum_B\sum_{k=1}^{3}\langle\Psi_I|\{\hat{P}_k,\delta^3(\mathbf{r}-\mathbf{r}_A)\}_+ \times\mathbf{e}_k|\Psi_J\rangle\langle\Psi_L|\hat{\Lambda}_{B,k}\mathbf{e}_k|\Psi_K\rangle. \quad (55)$$

The matrix elements entering this expression have already been evaluated in the framework of the LCAO approximation (34) and (35). Substituting the resulting forms (39) and (40) into (55), one obtains the final expression which completes the evaluation of the E_{pv} and its tensor components $E_{pv}^{i,j}$ in the framework of CIS for excited states:

$$E_{\mathrm{pv}}=\mathrm{Tr}\ E_{\mathrm{pv}}^{i,j}=E_{\mathrm{pv}}^{xx}+E_{\mathrm{pv}}^{yy}+E_{\mathrm{pv}}^{zz}, \tag{56}$$

$$E_{\mathrm{pv}}^{i,j}=-\frac{\alpha G_{\mathrm{F}}}{\sqrt{2}}\sum_{n}\ \frac{1}{E_0-E_n}\sum_{A}\ Q_{\mathrm{W}}^{c}(A)\sum_{I}\ \sum_{J}\ \sum_{K}\ \sum_{L}\ a_I^J(n)a_K^L(n)\sum_{B}\ \sum_{A'}\ \sum_{\mu'(A')}\ \sum_{B'}\ \sum_{\nu'(B')}\ C(I,A',\mu'(A'))$$

$$\times C(J,B',\nu'(B'))P(A,i|A',\mu'(A'),B',\nu'(B'))\sum_{A''}\ \sum_{\mu''(A'')}\ \sum_{B''}\ \sum_{\nu''(B'')}\ C(L,B'',\nu''(B''))C(K,A'',\mu''(A''))$$

$$\times\Lambda(B,j|B'',\nu''(B''),A'',\mu''(A'')). \tag{57}$$

A detailed description of the computer codes developed and used in our work can be found in Appendix A, appearing in PAPS.[76]

III. RESULTS AND DISCUSSION

A. E_{pv} for hydrogen peroxide in the framework of CIS-RHF

We started our calculations from hydrogen peroxide which has been studied previously by Mason and Tranter.[16] We have employed the same geometry (Fig. 2), but smaller steps in variation of the dihedral angle between two H–O–O planes to see the changes of E_{pv} in more detail. Hydrogen peroxide is a continuing subject of spectroscopic and theoretical studies,[77–81] for it exhibits a well-separated large amplitude motion: O–H torsion around O–O bond.

We discuss first the effect of the application of the CIS-RHF method on the magnitude of energy shifts due to parity violating weak interaction. From Table I one sees that both for 6-31G and for D95** basis sets the values of the diagonal tensor components E_{pv}^{xx} and E_{pv}^{zz} are well above $10^{-18}E_h$ though they are of different sign and thus cancelling each other, decreasing the overall value of E_{pv} by one order of magnitude. We will discuss the effect of the cancellation of tensor components and its relation to the geometry of the molecule and properties of E_{pv} in detail in the next section.

In spite of the competition of tensor components E_{pv}^{ii}, even for hydrogen peroxide the maximum values of total E_{pv} are well above $10^{-19}E_h$. We have found that the competition between different tensor components E_{pv}^{ii} is hidden in the representation of the total E_{pv} and seems to be a competition between contributions from different excited states. The contributions from the different excited CIS states come with different signs as already established in Ref. 12 at the SDE-RHF level when analyzing contributions from different molecular orbitals. A similar result applies for the CIS-RHF formalism as well. For illustration we have represented in Fig. 3 the contributions from different excited CIS states as bars with the full line representing the total E_{pv} as the number of the excited states increases. The dihedral angle of 120° has been chosen for this illustration, for other angles the picture is very similar. Large contributions of different sign come at low number n of excited states and they are much larger ($10^{-18}E_h$) than the net result which is one order of magnitude less ($10^{-19}E_h$) due to cancellation. It seems that the contributions of differents sign come without any obvious ordering. However, as the analysis presented in the next chapter will show, the competition of the contribution from the different excited states is nothing else but the competition

TABLE I. CIS-RHF for H_2O_2: tensor components E_{pv}^{ii} and total E_{pv} as functions of dihedral angle in units of $10^{-20}\,E_h$. Label I corresponds to the 6-31G basis set while label II corresponds to the D95** basis set.

Angle	$E_{\mathrm{pv}}^{xx}-I$	$E_{\mathrm{pv}}^{xx}-II$	$E_{\mathrm{pv}}^{yy}-I$	$E_{\mathrm{pv}}^{yy}-II$	$E_{\mathrm{pv}}^{zz}-I$	$E_{\mathrm{pv}}^{zz}-II$	$E_{\mathrm{pv}}-I$	$E_{\mathrm{pv}}-II$
0°	0.0	0.0	0.0	0.0	0.0	0.0	0.0	0.0
10°	−28.587	−37.333	0.8430	0.9898	18.768	23.895	−8.9761	−12.449
20°	−56.089	−70.369	2.7958	2.8606	36.938	46.146	−16.355	−21.362
30°	−80.816	−100.14	3.8768	4.5950	55.448	67.759	−21.491	−27.790
40°	−99.992	−122.96	4.7017	6.2507	72.238	88.240	−23.053	−28.471
50°	−114.64	−141.96	5.9140	7.3007	86.938	108.16	−21.785	−26.499
60°	−124.55	−154.00	6.3833	8.4482	99.950	124.25	−18.215	−21.297
70°	−128.77	−161.91	6.9562	8.9483	111.15	138.20	−10.660	−14.767
80°	−128.94	−162.54	7.5612	9.2629	118.66	148.98	−2.7138	−4.2907
90°	−125.73	−157.58	6.9199	10.494	124.56	155.70	5.7461	8.6147
100°	−118.71	−150.27	6.5778	9.7795	127.14	159.95	15.000	19.456
110°	−109.32	−138.02	5.7693	9.8489	125.25	157.20	21.702	29.031
120°	−98.463	−123.57	4.9507	8.7243	119.41	149.85	25.894	34.998
130°	−83.765	−106.38	4.1651	6.9171	109.19	136.07	29.588	36.610
140°	−68.782	−87.418	3.1285	5.3136	93.997	117.27	28.344	35.167
150°	−52.145	−66.708	2.3109	5.8440	74.331	94.095	24.497	33.231
160°	−35.502	−44.783	1.9380	3.4827	51.528	66.259	17.964	24.958
170°	−18.139	−22.131	1.3239	1.7224	27.322	33.000	10.507	12.591
180°	0.0	0.0	0.0	0.0	0.0	0.0	0.0	

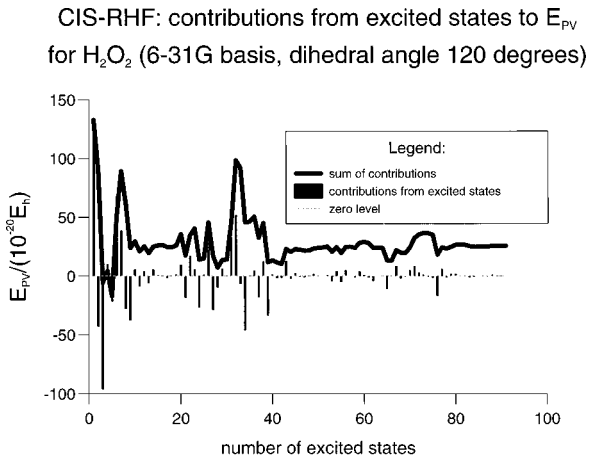

FIG. 3. H_2O_2. Contributions from the CIS excited states (bars) to the total E_{pv} (solid line) are shown as functions of the number of the excited CIS states, included into perturbation theory. The CIS-RHF calculation is done at a dihedral angle of 120° for the 6-31G basis set.

of the different tensor components E_{pv}^{ii}. The latter components contribute always with a certain sign but only for states of certain symmetry.

Figure 4 represents the results of a convergence analysis with respect to a change of the number of the CIS excitations included, with the dihedral angle being 120°. For GAUSSIAN92/94 CIS calculations using the frozen core approximation,[82] the maximum number of excited states for the 6-31G basis set is 91. Because the excitation energies from the core to the unoccupied valence orbitals are at least an order of magnitude larger than the intravalence excitation energies, the frozen core approximation is well justified. One sees that for sufficiently large CIS excitation energies (or sufficiently large denominators in perturbation theory) the contributions of highly excited states die out and the total

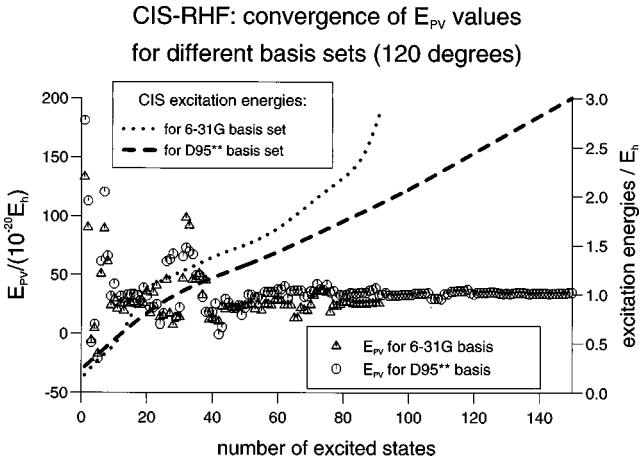

FIG. 4. H_2O_2. Convergence of the series of perturbation theory for E_{pv} with the number of the excited CIS states, included into the CIS-RHF calculation for two different basis sets: 6-31G (91 triangles) and D95** (150 circles). The corresponding energy denominators are also shown: dotted line for the 6-31G basis set and dashed line for the D95** basis. It is seen that numerical convergence (plateau) is achieved when the number of excited states becomes about 80 for the 6-31G basis set and about 90 for the D95** basis set. In both cases the excitation energy, at which the convergence is achieved, is about 2 eV.

E_{pv} approaches a steady horizontal line, indicating numerical convergence. The effect is even more pronounced for D95** basis set. The maximum number of excited states (217) was not used, because 150 excited states were sufficient for convergence. The convergence of separate tensor components E_{pv}^{ii} is similar and will be presented in the section devoted to the analysis of those tensor components. The same picture is found for the other dihedral angles in Table I. The convergence analysis along with the continuous behavior of the total E_{pv} and of its tensor components E_{pv}^{ii} let us conclude that the CIS-RHF calculations of ΔE_{pv} are consistent. The results presented here for ΔE_{pv} are much larger than reported before, using SDE-RHF, about equal to $10^{-20}E_h$, a figure which has customarily been cited.[30,83,84] Going just one step beyond the SDE-RHF formalism, to its natural generalization, CIS-RHF, one immediately gains an order of magnitude in ΔE_{pv} value. This raises a question about the magnitude of E_{pv} calculated in previous work done in the framework of the SDE-RHF approach.

The principal step in the improvement is to give up the single-determinant representation of the excitations. The qualitative difference between the SDE representation and the CIS representation is that the latter allows the excited states to be superpositions of the various single-electron excitations. This gives to the wave function of the excited state the necessary flexibility also with respect to the geometry changes. Since the parity violating electroweak interaction is determined by geometrical concepts, such as the absence of invariance under the reflection in space, it reacts sharply to the changes in the shape of the wave function. This sensitivity of E_{pv} has no analogues in other quantities of interest in quantum molecular physics, perhaps with the exception of circular dichroism.

B. E_{pv} for hydrogen peroxide in the framework of SDE-RHF

The main resource for improvement in the SDE-RHF approach is the change of size and quality of the basis set. We shall present here a systematic investigation (Fig. 5 and Table II). It has been shown before[16] that the 6-31G basis set provides stable results for E_{pv} in the sense that an extended basis set does not give values very different from those of the 6-31G basis set. The sequence of basis sets studied in Ref. 16, apart from minimal basis sets, was the sequence of split-valence bases: 4-31G→5-31G→6-31G→extended basis of 76 basis functions. Apparently, the main feature varied in Ref. 16 was the number of GTOs representing the single inner-shell function, except for the extended basis set.

The description of the derivation of the electrostatic potential used in Ref. 16 is lacking, which prevented us from exactly reproducing the conditions of calculations in Ref. 16. We attribute the modest differences between the SDE-RHF results obtained in our work and in Ref. 16 to the possible differences in electrostatic potentials used. Overall, the results of Mason and Tranter for hydrogen peroxide, calculated in the 6-31G basis, are in satisfactory agreement with our SDE-RHF results. In the second column of Table II we list only those conformations, where results are available from

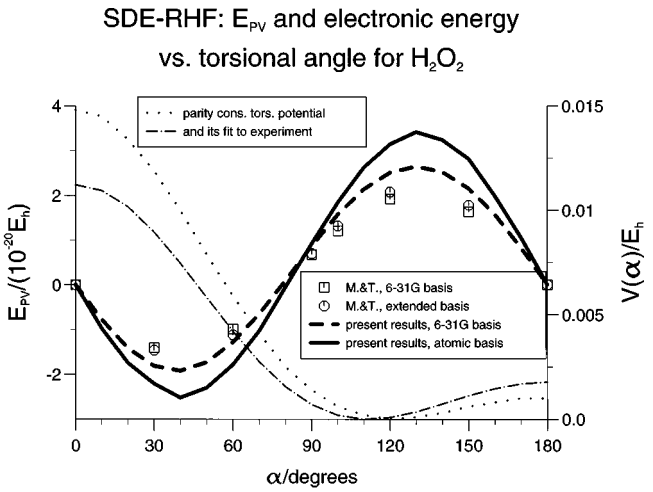

FIG. 5. H_2O_2. Comparison of the SDE-RHF results for total E_{pv} (left-hand scale), as a function of dihedral angle, obtained in this work (lines), with the results from the previous work (scattered markers) by Mason and Tranter Ref. 16. Results are compared for the 6-31G basis set (dashed line versus squares) and for the extended $(10s,6p;1d)$ basis set (solid line versus circles). The electronic energy (dotted line, right-hand scale) has been obtained for rigid geometries, specified in the text, at the 6-31G level. The experimental potential is from (Ref. 88).

Mason and Tranter. The first value corresponds to the 6-31G basis and the second to the extended basis set used in Ref. 16 (76 atomic orbitals for hydrogen peroxide: 11GTO-7GTO $11s$-$7p$ basis for oxygen atom and 3GTO-6GTO $3s$-$1p$ basis for hydrogen). A complete set of our data is available in Table C2 of Appendix C in the PAPS supplement.[76]

For larger basis sets our results show larger differences compared to the results of Mason and Tranter for their extended basis set. We studied the dependence of E_{pv} on the quality of the basis sets in more detail, varying not only basis size but also augmenting bases with polarization functions. Apart from the D95 and D95** basis sets[85] which are standard for GAUSSIAN92/94, we used the triple zeta basis[86] augmented with *d*-polarization function with exponents 0.85 for oxygen, and as an extended basis set the atomic basis by Huzinaga[87] with all GTOs uncontracted and again augmented with *d*-polarization function with exponents 0.85 for oxygen. The latter basis contains 84 basis functions for hydrogen peroxide. The relative difference in the values of E_{pv} in our work and in Ref. 16 for extended basis sets reaches 37% for 60°. Our calculations show that polarization functions affect E_{pv} values for torsional angles near maxima of torsional barriers for all basis sets considered. Near the maximum of the larger rotational barrier at 0° the polarization functions decrease the E_{pv}, while near the maximum of the lower rotational barrier at 180° polarization functions increase E_{pv}. Around the equilibrium torsional angle of 117° the polarization functions have no visible affect on E_{pv}. Another observation is that minimally uncontracting inner-shell functions, i.e., passing from split-valence bases to double zeta bases, changes E_{pv} up to 40% (6-31G and D95 bases at torsional angles above 100°). The 6-31G basis set employs just one contracted inner shell, while the D95 basis employs two contracted inner shells (split inner shell). This is the reason for the relatively poor performance of 6-31G calculations. Our results show that the 6-31G basis set should be rejected whenever size of the molecule and cost of evaluation allow it. At least, an attempt should be always made to uncontract inner-shell functions and to add polarization functions.

In the last column, together with E_{pv} values for the extended basis set, we list RHF energies of ground states for twisted geometries relative to the ground state energy for the optimized geometry. Note that for the sake of comparison with the previous work,[16] we have used the geometries exactly as used there. However, one has to remember that this geometry is different from the geometry obtained by means of the full optimization. The equilibrium RHF energy obtained by means of the full optimization is equal to $-150.8379E_h$ while correction to MP2 provides $-151.2573E_h$ after full optimization. The relative energies are given with respect to the RHF equilibrium energy. The changes in the torsional angle α are carried out with the rigid geometry which corresponds to the geometry used in Ref. 16. No partial optimization at different torsional angles has been carried out and thus the RHF energies reported cannot be regarded as the values corresponding to the proper minima of the potential. Figure 5 shows that our SDE-RHF results for hydrogen peroxide and the earlier results by Mason and Tranter are quite close for comparable basis sets

TABLE II. Hydrogen peroxide: SDE-RHF values of $E_{pv}/10^{-20}\ E_h$ for various basis sets and various torsion angles. In the second column the values from Ref. 16 are given when available. The first value corresponds to the 6-31 G basis and the second to the extended basis set from Ref. 16. The relative energies $\Delta E_{RHF}/E_h$ are given with respect to the RHF equilibrium energy.

Angle	M and T	6-31G	6-31G**	D95	D95**	TZ	TZ**	$(10s,6p;1d)$
30°	−1.40/−1.46	−1.813	−2.077	−2.235	−2.666	−2.588	−2.295	−2.205
								$\Delta E_{RHF}=0.0187$
60°	−0.98/−1.12	−1.281	−1.548	−1.601	−1.703	−1.855	−1.717	−1.781
								$\Delta E_{RHF}=0.0127$
90°	0.68/070	0.868	0.940	1.041	1.083	1.093	1.109	0.923
								$\Delta E_{RHF}=0.0082$
120°	1.92/2.08	2.513	2.928	3.151	3.357	3.435	3.377	3.147
								$\Delta E_{RHF}=0.0068$
150°	1.64/1.78	2.155	2.551	2.720	2.933	2.968	2.921	2.820
								$\Delta E_{RHF}=0.0074$

though our results are in average about 20% higher. The electronic potential energy is also given as a function of the torsional angle. It is interesting that the dependence of the total E_{pv} on the dihedral angle exhibits additional crossing of zero, apart from achiral limits defined by the geometry of the molecule itself. However, it must be stressed that there are no physical reasons determining zeros of the E_{pv} values at chiral geometries. It is therefore instructive to study the structure of the total E_{pv} in more detail in the following section.

C. Effect of mutual cancellation of diagonal components of the E_{pv} tensor for H_2O_2

We discuss here an effect, which can be found in both the CIS-RHF and in the SDE-RHF frameworks, but has been previously overlooked: the effect of mutual cancellation of the diagonal tensor components of E_{pv}. The total E_{pv} entering both (33) and (55) is a composite quantity which carries only one spatial index: it is the index of the vector components of the momentum operators and of the angular momentum operators of the electrons in the molecules. We now show that the reason for the existence of the ''strange chiral zeros'' of the total E_{pv} lies in the mutual cancellation of the diagonal tensor components of E_{pv}, the effect which is clearly seen in both CIS-RHF and in SDE-RHF formalisms, though these different formalisms give order-of-magnitude different values for both the tensor components and the total values of E_{pv}.

The diagonal tensor components E_{pv}^{ii} for hydrogen peroxide are well above $10^{-18}E_h$ which is two orders of magnitude greater than the typical figure accepted before, $10^{-20}E_h$. However, the total value of E_{pv} is only about $10^{-19}E_h$, which is one order of magnitude lower than the values of the diagonal tensor components, because of considerable mutual cancellation of the diagonal tensor components of the E_{pv}.

As we see from Figs. 6(a) (CIS-RHF at 6-31G level) and 6(b) (CIS-RHF at D95**) and Table I, the tensor components E_{pv}^{ii} are always different from zero at chiral geometries. They vanish at achiral geometries. The components may have different signs.

At the standard orientation of the coordinate system used by GAUSSIAN92/94 (see Fig. 2), the main competing components are E_{pv}^{xx} and E_{pv}^{zz} while the E_{pv}^{yy} component is almost two orders smaller than these large components. The y axes of the coordinate system is directed along the O–O bond and the dihedral angle between two molecular planes H–O–O and O–O–H is bisected by the yOz plane. The only symmetry element for a nonplanar geometry of hydrogen peroxide is the rotation by angle π about the C_2 symmetry axis (z axis). The CIS excited states, which must be triplets to make a nonzero contribution to E_{pv}, are either of A or B symmetry in the C_2 point group.

It is, however, clear that this symmetry operation does not alter the sign of the z component of the momentum operator and changes the signs of its x and y components. Similarly, there is no effect of C_2 transformation on the z component of the angular momentum operator while its x and y components change their signs.

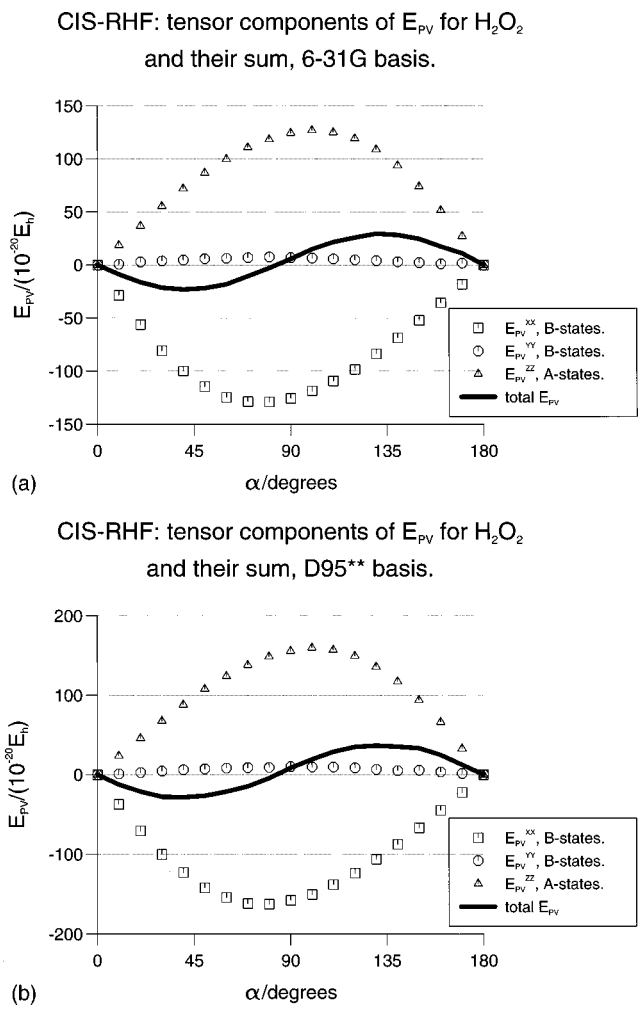

FIG. 6. H_2O_2. The dependences on the dihedral angle are shown for the diagonal tensor component values E_{pv}^{xx} (squares), E_{pv}^{yy} (circles), and E_{pv}^{zz} (triangles), as well as for the total values of E_{pv} (solid line). Only states of certain symmetry contribute to separate tensor components: B-states: to E_{pv}^{xx} and E_{pv}^{yy} and A-states: to E_{pv}^{zz}. (a) The method is CIS-RHF at the 6-31G level. (b) The method is CIS-RHF at the D95** level.

Since the ground state is of A symmetry, the excited states of A symmetry contribute only to E_{pv}^{zz} and the excited states of B symmetry contribute only to E_{pv}^{xx} and E_{pv}^{yy}. The numerical results are in perfect agreement with this selection rule (this is illustrated in Table C1 of the PAPS supplement[76]).

Figure 7 illustrates the convergence of the E_{pv}^{ii} with the increase of the number of the excited CIS states included into calculation by showing the dependence of the tensor components on the number of excited states included for 6-31G and D95** basis sets at dihedral angle 120°. One sees that the convergence is good in the case of 6-31G basis and excellent in the case of D95** basis.

The calculations which have been carried out with the D95** basis set allowed us to trace the hydrogen contributions. We found that both in CIS-RHF and, of course, in SDE-RHF formalisms the hydrogen contributions are at least four orders of magnitude smaller than those from oxygen. Figure 8 illustrates this fact. The typical order of magnitude of the tensor components is $10^{-23}E_h$ while for oxygen it is

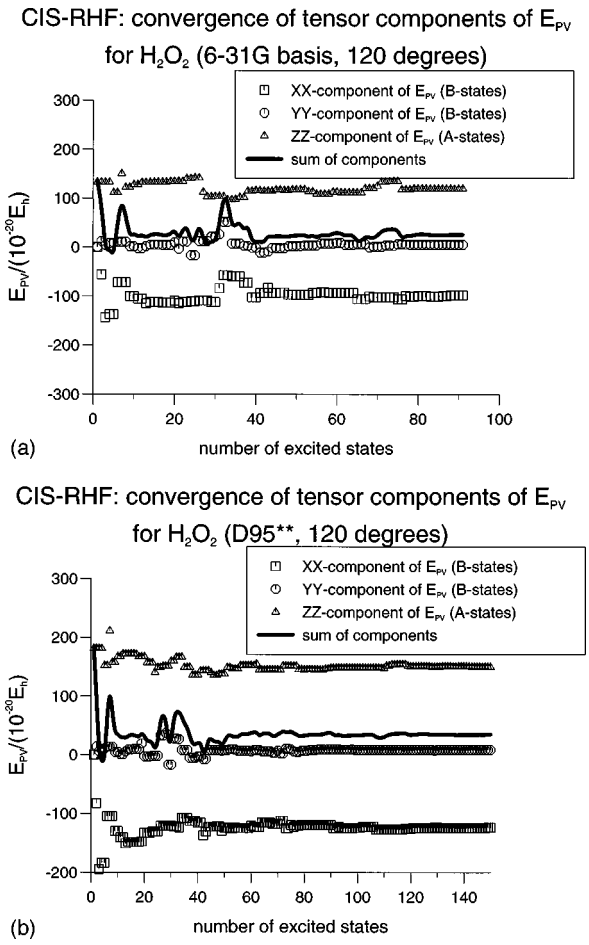

FIG. 7. H_2O_2. Illustration to the very smooth character of the convergence of perturbation theory for separate diagonal tensor components E_{pv}^{xx} (squares), E_{pv}^{yy} (circles), and E_{pv}^{zz} (triangles). The method of calculation is CIS-RHF, dihedral angle is fixed at 120°. (a) The basis set is 6-31G. (b) The basis set is D95**.

$10^{-18}E_h$. The oscillations are negligible on the scale of the E_{pv} for oxygen atoms.

The effect of the mutual cancellation of the diagonal tensor components of E_{pv} is also clearly seen in the framework of the SDE-RHF formalism. Figure 9 shows the behavior of the tensor components as the dihedral angle varies. For illustration we have chosen the 6-31G basis set, which makes the picture directly comparable with previous work. The tensor components are very well separated even within SDE-RHF calculations, respecting the chiral geometry of twisted conformations of hydrogen peroxide. They become zero only at achiral geometries.

D. Study of H_2S_2

1. Introductory discussion of the Z dependence of E_{pv}

An important property of the matrix element of the parity violating interaction (15) is its dependence on the charge Z of the atomic nucleus.

As has been shown in Ref. 62, the matrix element of the parity violating weak interaction (15), taken between atomic wave functions, has a Z^3 or slightly stronger dependence on Z, if one takes into account relativistic correction. For atoms

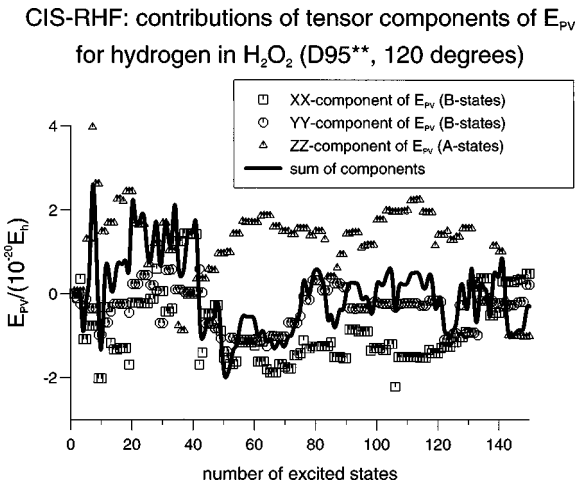

FIG. 8. Illustration to the oscillatory character of the series of perturbation theory for hydrogen contributions to tensor components of E_{pv} as functions of the number of the excited CIS state, included into the CIS-RHF calculation for the D95** basis set (150 points). Note the scale chosen for hydrogen contributions which is three orders of magnitude smaller than the one for oxygen contributions in the previous figures.

of the first and the second rows of the periodic table the relativistic correction can be neglected. The cubic overall dependence on Z results from the $Z^{3/2}$ dependence of the Coulombic wave function at the nucleus and the $Z^{1/2}$ dependence of the derivative of this wave function at the nucleus together with a factor of Z which enters the expression (16) for the electroweak charge, derived on the basis of the standard model.[4–6] For molecules it has been argued in Ref. 12 that the matrix element of the leading parity violating term (15), taken now between molecular wave functions, acquires an additional factor $\alpha^2 Z^2$. The latter is the ratio of the matrix element of the spin-orbit coupling to the excitation energy. Such a ratio is exact only for a hydrogen atom and is subject to be influenced by the screening of the electrostatic potential in many-electron atoms.[66,73,74] While this additional factor decreases the matrix element of the parity violating weak interaction (15) by at least α^2 in the case of molecules compared with atoms at the same Z, it is believed[12] that with

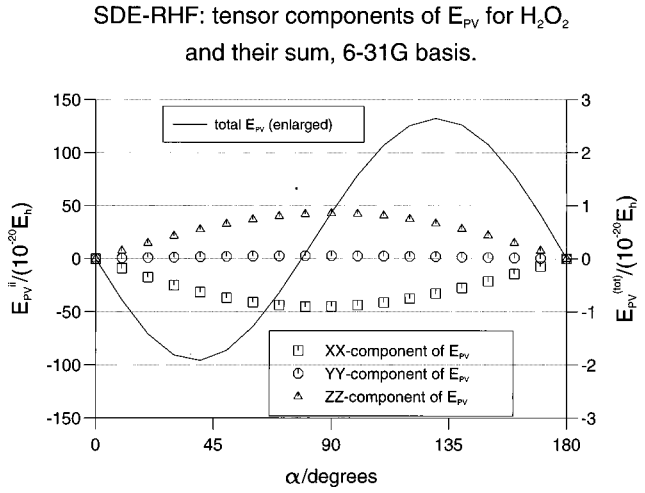

FIG. 9. Tensor components E_{pv}^{ii} within SDE-RHF for H_2O_2. 6-31G basis set.

TABLE III. Hydrogen disulphide: SDE-RHF values of $E_{pv}/(10^{-20}\,E_h)$ for various basis sets and various torsion angles. In the second column the E_{pv} values, obtained from Ref. 16 at the 4-31 G level are given when available. The relative energies $\Delta E_{RHF}/E_h$ are given with respect to the RHF equilibrium energy.

Angle	M and T (4-31G)	4-31G	6-31G	6-31G**	D95	D95**
30°	−134.0	−145.140	−195.136	−187.806	−160.391	−171.606
						$\Delta E_{RHF}=0.010\,07$
60°	−136.0	−147.880	−196.446	−188.254	−161.876	−171.873
						$\Delta E_{RHF}=0.003\,12$
90°	−44.9	−49.158	−65.389	−63.498	−52.715	−56.568
						$\Delta E_{RHF}=0.000\,00$
120°	49.7	53.185	67.896	62.4458	58.756	59.699
						$\Delta E_{RHF}=0.001\,93$
150°	67.2	72.375	92.725	86.358	79.000	81.154
						$\Delta E_{RHF}=0.005\,72$

increasing Z this additional factor brings an approximate Z^2 dependence on top of the known atomic Z^3 dependence.

We study here the effect of increasing Z on the value of E_{pv} by comparing hydrogen peroxide H_2O_2 and hydrogen disulphide H_2S_2 over the whole range of the dihedral angle. Our study differs from an earlier one[16] by the method of calculation (both SDE-RHF and CIS-RHF) and by considering the tensor character of the E_{pv}. Indeed, there are ranges of the values of the dihedral angle at which the values of the total E_{pv} for hydrogen peroxide H_2O_2 and for hydrogen disulphide H_2S_2 cannot be compared meaningfully because within these ranges the total E_{pv}'s for these molecules have different signs. In Ref. 16 the comparison was done by plotting the total E_{pv} for hydrogen peroxide H_2O_2 and for hydrogen disulphide H_2S_2 on the same graph but at scales differing by factor $2^5=32$. This generated the impression that for the total E_{pv} there is even greater than Z^5-fold increase. Thus the authors of Ref. 16 concluded that the ratio of these values is ''... above the expected Z^5 ratio, which remains exceeded... over the major part of the dihedral-angle range.'' This was perhaps the reason which lead some authors to state that there is even Z^6 amplification of E_{pv}.[89] These assumptions are erroneous.

As we have discussed, the total E_{pv} should not be used for deriving the dependence on Z. What must be compared are the tensor components. These components give very stable ratios over the whole conformational range for the dihedral angle, from 0.0° to 180.0°. As more accurate CIS-RHF calculations show, the Z exponents of ratios are always less than 5.0, but larger than 3.0.

We shall refer to this as the $Z^{3+\delta}$ law. Hence our task is to establish the value of δ, which carries all the molecular amplification effects in absence of an external field, while the exponent 3.0 is an atomic effect as was shown in Ref. 62.

We will show below that at the standard orientation of the Cartesian coordinate axes (Fig. 2) the values of the exponents are 4.403 ± 0.061 for the E_{pv}^{xx} component and 4.445 ± 0.048 for the E_{pv}^{zz} component. The latter two components are the largest components, they essentially determine the value of the total E_{pv} and the extent of their mutual cancellation is very high. Therefore for the E_{pv}^{xx} component and for the E_{pv}^{zz} component the molecular exponent δ takes the values from the intervals defined as 1.403 ± 0.061 and 1.445 ± 0.048, respectively.

The two values for the E_{pv}^{xx} component and for the E_{pv}^{zz} component are the same within the standard error. The ratio and the exponent for the E_{pv}^{yy} component, which is two orders of magnitude smaller than the other components, are subject to large fluctuations and the value obtained, $\delta=2.233\pm0.395$, cannot be considered to be a reliable result. One has also to note that the detailed comparison of the ratios of tensor components values and of their logarithms over the whole conformational range practically excludes from consideration the molecular asymmetry factor η[10,12,16] and attributes all Z-depending enhancement properties to the single quantity, to the exponent δ of the molecular E_{pv}.

2. Total E_{pv} and its diagonal tensor components for H_2S_2 in SDE-RHF and in CIS-RHF formalisms

We have employed the same geometry of the H_2S_2 as in Ref. 16. The S–S and S–H bond lengths were taken equal 2.055 Å and 1.352 Å, respectively, and S–S–H bond angle equal to 92.0° (see also Ref. 90 for a detailed spectroscopic investigation). The dihedral angle has been varied over the same range with the same step as for hydrogen peroxide. E_{pv} values, along with those obtained in Ref. 16), are summarized in Table III (more complete data can be found in Tables C3 and C4 in the PAPS supplement,[76] the latter containing tensor components). The corresponding changes in the electronic potential over the conformational range considered are taken from calculations with D95** basis set (the last column in Table III). As is seen from the second and the third columns in Table III, our SDE-RHF results for hydrogen disulphide at the 4-31G level are in agreement with the results obtained by Mason and Tranter,[16] where these are available. The remaining difference of about 10% is to be attributed, as in the case of hydrogen peroxide, to the possible difference in the methods of evaluation of the electrostatic potential for spin-orbit coupling. All the high-quality basis sets used, 6-31G, 6-31G**, D95, D95**, give the maximum SDE-RHF values of E_{pv} for hydrogen disulphide at 40° ($217.435\times10^{-20}E_h$, 6-31G basis) while the 4-31G basis gives the largest value at 50° ($162.503\times10^{-20}E_h$). The

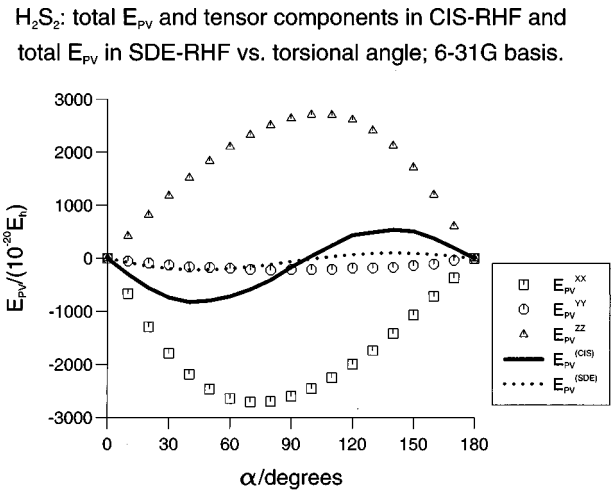

FIG. 10. Hydrogen disulphide, 6-31G basis set. For CIS-RHF, the total E_{pv} (full line) and the tensor components E_{pv}^{ii}, $i=x,y,z$, are shown as functions of dihedral angle. For SDE-RHF, only the dependence of the total E_{pv} on the dihedral angle is shown (dotted line).

gain in E_{pv} due to the improvement in the quality of the basis set within the SDE-RHF formalism is about 34%.

The application of the CIS-RHF method to hydrogen disulphide brings a substantial increase in the total E_{pv} of about a factor 4 at 40° for the 6-31G basis set, $8.271\times10^{-18}E_h$ for CIS-RHF versus $2.174\times10^{-18}E_h$ for SDE-RHF. The results are visualized in Fig. 10, when CIS-RHF results are compared to SDE-RHF results (Table C5 in Appendix C of the PAPS supplement[76] contains a complete set of numerical data). The CIS-RHF perturbation series for the E_{pv} for hydrogen disulphide reveals smooth convergence at the CIS(frozen core)/6-31G level of theory. As is seen from Fig. 11, the series converges at about 50–60 excited states included in the calculation. The excitation energy is there just half of its maximum. Therefore the CIS-RHF results on hydrogen disulphide are considered as reliable (within the method used). The E_{pv}^{zz} value of $-2.710\times10^{-17}E_h$ at 100° is

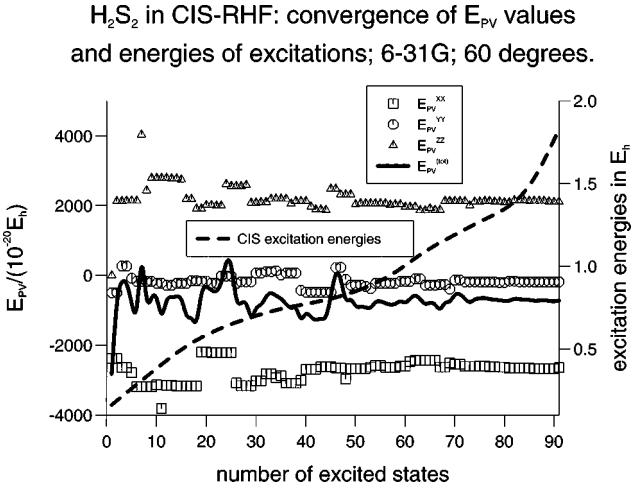

FIG. 11. The CIS-RHF (frozen core, 6-31G basis set) perturbation series for the E_{pv} for hydrogen disulphide reveales smooth convergence at about 50–60 excited states included in the calculation, where the excitation energy reaches about a half of its maximum value.

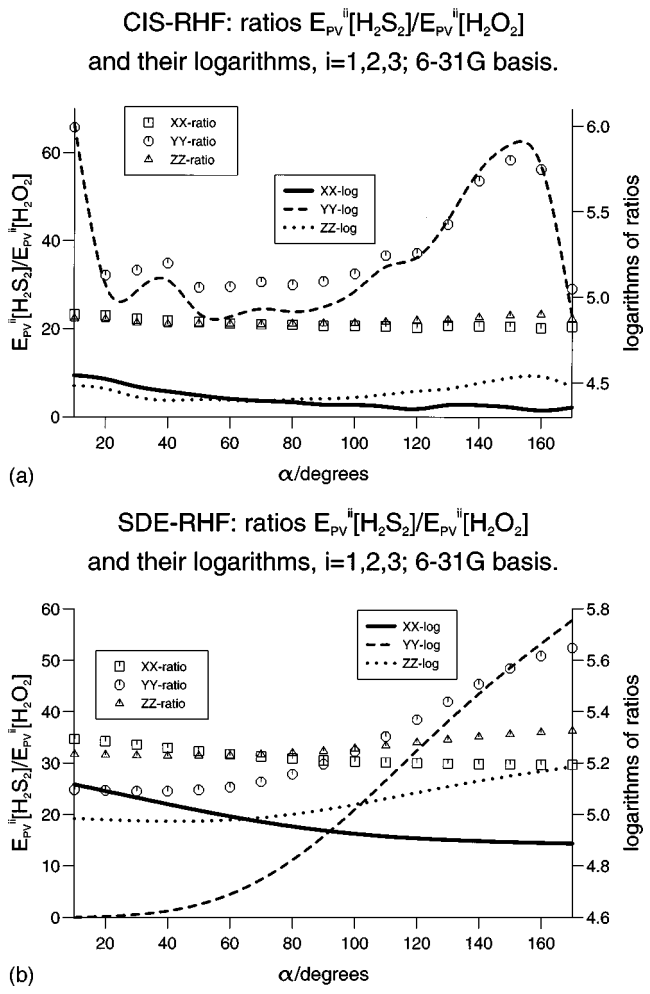

FIG. 12. The ratios $E_{\mathrm{pv}}^{ii}[\mathrm{H_2S_2}]/E_{\mathrm{pv}}^{ii}[\mathrm{H_2O_2}]$, $i=x,y,z$, and their logarithms calculated with the 6-31G basis set, (a) by the CIS-RHF method; (b) by the SDE-RHF method.

so far the largest known figure obtained within a reliably tested procedure. The total E_{pv} value of $8.271\times10^{-18}E_h$ exceeds by more than a factor of 2 the E_{pv} obtained in Ref. 28 when scaled to a single sulphur atom.

3. E_{pv} for H_2S_2 versus E_{pv} for H_2O_2

We are now set to undertake a quantitative check of the $Z^{3+\delta}$ amplification law within the CIS-RHF procedure. As already stated, the quantitative comparison of the total E_{pv} through the logarithms of their ratios is not possible, because there are ranges of the torsional angle where the E_{pv} of H_2S_2 and the E_{pv} of H_2O_2 have different signs. For the total E_{pv}'s obtained within the CIS-RHF method this range is approximately from 85° to 95° while for the SDE-RHF method such a range is much larger, between 75° and 105°.

In contrast to this, the tensor components E_{pv}^{ii}, $i=x,y,z$, have definite signs in given conformational ranges. The ratios of the E_{pv}^{ii}, $i=x,y,z$, for H_2S_2 and for H_2O_2 within the CIS-RHF method and the corresponding logarithms are shown in Fig. 12(a). The stability for the leading E_{pv}^{xx} and E_{pv}^{zz} components is outstanding. The ratio for E_{pv}^{xx} is in the very narrow interval 21.168 ± 0.915 (logarithm $=4.403\pm0.061$). For the E_{pv}^{zz} the ratios are within 21.794

± 0.734 (logarithm $= 4.445 \pm 0.048$). The results on the E_{pv}^{yy} component should be disregarded, since they are ratios of small numbers which are two orders of magnitude smaller than for the leading E_{pv}^{xx} and E_{pv}^{zz} components. Indeed, the deviation of the results for E_{pv}^{yy} is large: the ratios are within the interval 39.056 ± 11.910 (logarithms are within the interval 5.233 ± 0.395). Table C6 of the PAPS supplement[76] contains a complete set of numerical data.

For purposes of comparison we present in Fig. 12(b) (numerical data in Table C7 of the PAPS supplement[76]) the ratios and the corresponding logarithms, obtained within the SDE-RHF formalism. The general trend in comparison with the CIS-RHF results is that the values are much less stable, and they are scattered over wider intervals. For the leading E_{pv}^{xx} and E_{pv}^{zz} components one gets, respectively, the ratios within the intervals 31.259 ± 1.699 and 33.096 ± 1.780, and the logarithms within the intervals 4.964 ± 0.077 and 5.047 ± 0.077. For the smallest E_{pv}^{yy} the ratio and its logarithm are most scattered: the intervals are 33.964 ± 10.223 and 5.028 ± 0.414.

We find, by means of the direct quantitative analysis of the mean values of the tensor components of the parity violating interaction, that the exponent δ in the molecular Z dependence of E_{pv} never reaches the value 3.0, and most probably is well below 2.0. Our most reliable results obtained on the basis of the analysis of the leading tensor components provide the following values of δ within the reliable CIS-RHF procedure: 1.403 ± 0.061 (from the data on E_{pv}^{xx}) and 1.445 ± 0.048 (from the data on E_{pv}^{zz}), which is the same within the confidence intervals (Table C6 of the PAPS supplement[76]).

The SDE-RHF method gives the somewhat higher values of δ on the basis of the analysis of the leading tensor components: 1.964 ± 0.077 and 2.047 ± 0.077. These values are very close to 2.0. However, the dependence of the molecular E_{pv} on Z comes from the ratio of the matrix element of the spin-orbit coupling to the excitation energy.[12] The dependence of this matrix element on Z is determined, in particular, by the Z dependence of the electrostatic potential. While such a potential behaves as Z/r at the nucleus, it is just $Z^0/r = 1/r$ outside the core. Therefore the mean value of the electrostatic potential exhibits some Z^{σ} dependence, where σ is a number between 0 and 1. That means that the pure Z^2 dependence of the spin-orbit matrix element holds only for hydrogen, while for the many-electron atoms it is somewhat weaker: only $Z^{1+\sigma}$, $0.0 < \sigma < 1.0$. Our CIS-RHF calculations indicate that $\delta \approx 1.5$ and hence a plausible value of $\sigma \approx 0.5$. The maximum value $\sigma = 1.0$, which would be consistent with the SDE-RHF results, is not considered to be plausible.

E. Total E_{pv} and diagonal tensor components E_{pv}^{ii} for N_2O_4 in both formalisms

In order to try to utilize the $Z^{3+\delta}$, $\delta \approx 1.5$, dependence of the E_{pv}, one might look at N_2O_4, which consists of ''heavy'' atoms only. One can expect an increase of the overall E_{pv} value which will be proportional to the increase in charge and to the number of the heavy atoms. However, the extent

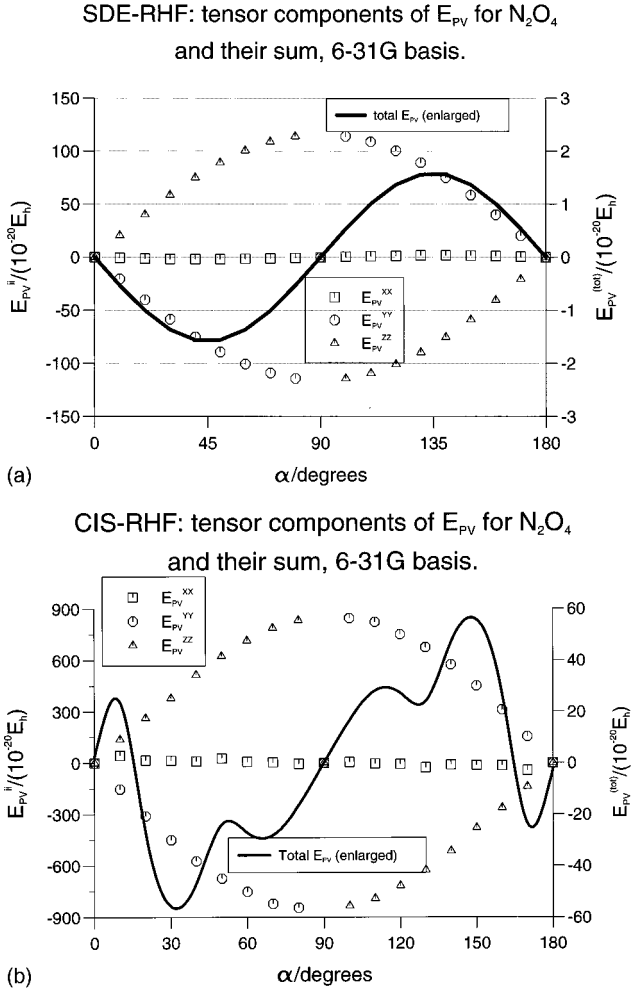

FIG. 13. N_2O_4. (a) Diagonal tensor components of E_{pv} in the framework of the SDE-RHF approach for the 6-31G basis set. On the scale of variation of the tensor components (markers) the total E_{pv} (solid line) is negligible. This illustrates the highest degree of the mutual cancellation of diagonal tensor components of E_{pv} in zero external field. (b) The same as in (a) but for CIS-RHF formalism. The axes definitions are as follows: X axis goes through nitrogen atoms while Y and Z axes bisect dihedral angles for each of the oxygen atoms belonging to different NO_2 groups. It is clear that either Y axis or Z axes can be chosen as the main symmetry axis.

of the mutual cancellation of the diagonal tensor component E_{pv}^{ii} for N_2O_4 is astounding. This is illustrated by the SDE-RHF evaluation of the tensor components at the 6-31G level. As is shown in Fig. 13 the components E_{pv}^{ii} easily reach $10^{-18}E_h$ while after summing them up one ends up just with $10^{-20}E_h$. The higher extent of the mutual cancellation is connected with the higher symmetry of this molecule, the full point group is D_2 in comparison with C_2 in the case of hydrogen peroxide. The higher symmetry is also reflected by the fact that the tensor components change abruptly near 90° while their sum, the total E_{pv}, behaves quite smoothly, Fig. 13(a) (numerical data in Table C8 of the PAPS supplement[76]). The coordinate axes for this molecule are defined so that the X axis goes through nitrogen atoms while Y and Z axes bisect dihedral angles for each of oxygen atoms belonging to different NO_2 groups. It is clear that either Y axis or Z axis can be chosen as the main symmetry axis.

Employing the CIS-RHF formalism for the evaluation of

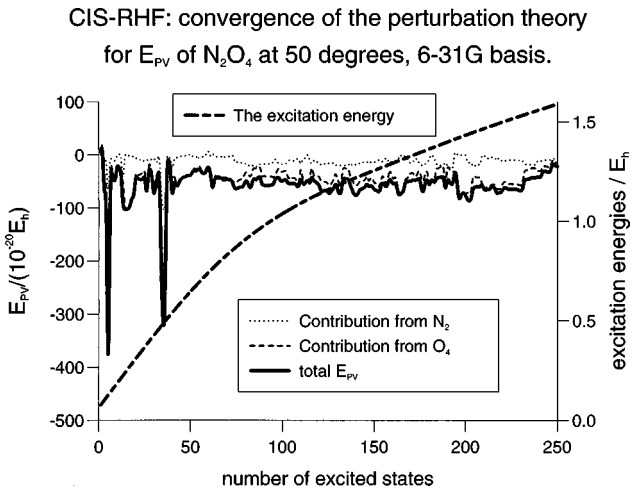

FIG. 14. N_2O_4. Illustration to the convergence of perturbation theory for the total molecular E_{pv} as well as for separate atomic contributions from N_2 (dotted line) and O_4 (dashed line). The method of calculation is CIS-RHF, the dihedral angle is fixed at 50°, the basis set is 6-31G.

the tensor components does not alter the qualitative behavior of E_{pv}^{ii}. The same stepwise change at 90° takes place though the maximum of the E_{pv}^{ii} increases and reaches $8.448 \times 10^{-18} E_h$ at 80° as is shown in Fig. 13(b). One reason why the total E_{pv} value is not smooth as a function of the dihedral angle in the CIS-RHF framework could be that the perturbation theory shows weak convergence. This is illustrated in Fig. 14 where it is seen that the number of CIS states included into the current calculation (250) is not sufficient for complete convergence. The reason for the relatively low value of the total E_{pv} for N_2O_4 may be that this molecule possesses an unusually long N–N bond length (177 ± 2 pm[91]). The resulting decrease of the intensity of the spin-orbit interaction leads, in turn, to a decrease of E_{pv}.

We have employed for our calculations of E_{pv} the *ab initio* (MP2) geometry which gives the value of the N–N bond length as 178.6 pm (Ref. 91, Table I). The rigid geometries for the different torsional angles were otherwise fixed at this geometry when systematically increasing the basis size and varying the exponents of the GTO basis functions. It would be desirable to go beyond the single-determinant approach for N_2O_4.[92,93]

The values of total E_{pv} for N_2O_4 in the framework of SDE-RHF (Table IV) are even somewhat less than those for the H_2O_2 molecule. So one can speak of the competing interatomic distance factor which is to compensate the advantageous $Z^{3+\delta}$, $\delta \approx 1.5$, dependence of total E_{pv}. Since all atoms contribute to the total E_{pv}, the table lists all separate atomic contributions and the overall contribution for the given geometry and for the given basis. The overall value of the total E_{pv} is expressed through the atomic values of two nitrogen atoms E_{pv}^{N} and of four oxygen atoms E_{pv}^{O}, according to the simple additive formula $E_{pv}^{tot} = 2E_{pv}^{N} + 4E_{pv}^{O}$. Furthermore, even in the framework of SDE-RHF the total E_{pv} for the N_2O_4 molecule vanishes only at achiral geometries, i.e., only when the dihedral angle is equal to zero or it is an integer multiple of 90°. Since both the Y axis and Z axis are symmetrically equivalent (either of them can be chosen as the main symmetry axis), the components E_{pv}^{yy} and E_{pv}^{zz} behave practically symmetrically and cancel each other very precisely as it is seen from Fig. 13 and Table C8 of the PAPS supplement.[76] So, only the E_{pv}^{xx} component survives to provide the total E_{pv}. For symmetry reasons, the parity violating potentials at $(90° + \alpha)$ and at $(90° - \alpha)$ have the same magnitude but the opposite signs.

We found no dependence of the sign of E_{pv} on the choice of the basis set in the SDE-RHF framework. Again, the inclusion of the polarization functions seems to be important since for all the basis sets under consideration the inclusion of the polarization functions leads to better agreement of E_{pv} values with the value obtained for the extended basis set. While the simplest modification of the core functions for the D95** basis decreases E_{pv} (compared to the one for the 6-31G** basis) the further uncontraction to TZ** leads to a sufficient increase, close to the value for the extended basis set. The heavier the atoms contributing to E_{pv}, the more flexibility should be allowed for the core functions when uncontracting them.

The example of the N_2O_4 molecule shows that one cannot just rely on the $Z^{3+\delta}$ dependence of E_{pv}. Structural factors such as bond lengths can decrease or even fully compensate the increase of the E_{pv} expected from the $Z^{3+\delta}$ law. Nevertheless, for the CIS-RHF method, for instance, E_{pv}^{zz} for N_2O_4 reaches $8.44 \times 10^{-18} E_h$ at 80°. Because of the mutual cancellation of the diagonal tensor component E_{pv}^{ii} for N_2O_4 the total E_{pv} for N_2O_4 has its maximum value at 30° and 150°, reaching $5.574 \times 10^{-19} E_h$ in absolute value (Table C10 of the PAPS supplement[76]). In contrast to SDE-RHF results, this maximum total E_{pv}, obtained within CIS-RHF, is larger

TABLE IV. N_2O_4: SDE-RHF values of $E_{pv}/10^{-20}$ E_h for various basis sets and various torsion angles. The total parity violating energy E_{pv}^{tot} of the N_2O_4 molecule is expressed through atomic contributions E_{pv}^{N} and E_{pv}^{O} as follows: $E_{pv}^{tot} = 2E_{pv}^{N} + 4E_{pv}^{O}$. At 0° and 90° all atomic contributions vanish identically because of symmetry reasons. More complete data are in Table C9 of the PAPS supplement (Ref. 76).

Angle	at. and mol.	6-31G	6-31G*	D95	D95*	TZ	TZ*	(10s, 6p;1d)
30°	N	0.130	0.261	0.490	0.414	0.271	0.163	0.136
	O	−0.407	−0.531	−0.539	−0.519	−0.518	−0.563	−0.551
	N_2O_4	−1.367	−1.603	−1.177	−1.248	−1.530	−1.926	−1.932
60°	N	0.089	0.233	0.374	0.382	0.230	0.137	0.110
	O	−0.387	−0.494	−0.538	−0.487	−0.492	−0.545	−0.535
	N_2O_4	−1.369	−1.511	−1.407	−1.185	−1.508	−1.904	−1.921

than the corresponding maximum total E_{pv} for hydrogen peroxide.

F. Analysis of the limitations of both formalisms

Both the CIS-RHF and SDE-RHF formalisms are subject to limitations for certain molecules due to their complex electronic structure or because of geometrical effects. We shall discuss here briefly some of the limitations with the sequence of molecules C_2H_2, C_2H_4, C_2H_6. For a full account of numerical results and the relevant detailed discussion in connection with these we refer to Appendix B in the PAPS supplement.[76] The equilibrium geometries of all three molecules are achiral, however, vibrational excitation and distortion from equilibrium generate chiral geometries.[39] For ethylene we have carried out calculations on E_{pv} as a function of torsional angle, α, which are comparable to those of Refs. 12 and 16. While we have reproduced the earlier results and extended them to larger torsional angles and to CIS-RHF, the improvement achieved over previous results are only modest, because both types of formalisms are inadequate, certainly at large torsional angles close to 90°. One finds generally a smooth rise of E_{pv} and a sudden jump to similar values of opposite sign when crossing the transition state at 90°. While the behavior in CIS-RHF is somewhat smoother and more realistic, we still consider it inadequate. At 90° the π and π^* orbitals become degenerate and the two determinants for the ground state ^1A_g and for the doubly excited state $^1A_g^*$, $(\pi)^2 \rightarrow (\pi^*)^2$, have to be combined into the wave function of D_{2d} symmetry, thus requiring a multiconfigurational wave function.[94,95] Ethylene is clearly a case where one must go beyond both the CIS-RHF and SDE-RHF approaches in order to obtain reliable E_{pv} at large torsional angles close to 90°. An interesting finding from the CIS-RHF calculations for small angles is that all tensor components have the same signs in this case and there is no cancellation of their contributions. At a torsional angle of 30° the E_{pv} for SDE-RHF is $2.6\times10^{-20}E_h$ and for CIS-RHF it is $3.1\times10^{-20}E_h$ (both for D95** basis set).

For acetylene we have carried out calculations at structures similar to those for ethylene, but with two hydrogens removed. These structures are far away from the equilibrium geometry of acetylene but also qualitatively comparable to H_2O_2 and thus useful for various comparisons. In SDE-RHF calculations with various basis sets we find a smooth behavior of E_{pv} as a function of torsional angle over the full conformational range for one enantiomer. The value at 30° is $3.0\times10^{-20}E_h$ and reaching a maximum in absolute value at 60° ($-3.6\times10^{-20}E_h$, both with D95** basis set). These values are comparable to those for H_2O_2 and ethylene at similar distortions and level of calculations. There are zero values for E_{pv} in acetylene at torsional angles corresponding to chiral geometries (see Table C14 in the PAPS supplement[76]). Although there are no particularly artificial features observed in E_{pv}, because of the electronic structure of acetylene being even more complex than that of ethylene, neither CIS-RHF nor SDE-RHF results are expected to be close to definitive values.

Ethane shows a different problem. Its electronic ground-state structure is simple at all torsional angles and thus should be amenable to CIS-RHF calculations for E_{pv}. However, the conformational range of chiral geometries between sets of achiral geometries covers only 60° in this case for symmetry reasons (disregarding other distortions). It seems that this introduces an almost cylindrical, effectively achiral, symmetry for the electronic wave function, as we find that the values of E_{pv} are very small (about $0.1\times10^{-20}E_h$ at most) depending erratically (even in sign) upon basis set size and computational method although the behavior as a function of torsional angle is smooth for any given theoretical method. It seems that the approaches are not adequate to calculate such small values of E_{pv} in a stable fashion.

G. Numerical illustration to the single-center theorem: Methane

Due to the specific structure of Eq. (41) and due to the vector properties of the angular momentum, only those matrix elements of the electroweak effective interaction and of the spin-orbit interaction survive which arise from different atomic centers.[12] The matrix elements $P(A,k|\mu'(A),\nu'(A))$ and $\Lambda(B,k|\nu''(B),\mu''(B))$ in Eqs. (46) and (47) confined to the same center ($A=B$) give contributions to E_{pv} which are mutually canceling each other during the summation over the vector index k in Eq. (44). The statement is exact if one uses a minimal basis set, as the only contribution to E_{pv} in the case of a minimal basis set comes from matrix elements with $A\neq B$ in Eq. (44). This was called the ''single-center theorem''.[12] An immediate consequence of this is that a molecule, possessing a single heavy atomic center, will have zero E_{pv} in the minimal basis set or perhaps a small E_{pv} for an extended basis set. Larger E_{pv} arise in molecules with more than one heavy atomic center. This consideration is particularly valid for SDE-RHF wave functions.

It is instructive to provide a numerical example for the case of extended basis sets in order to illustrate the single-center theorem and to trace the actual reduction of the E_{pv} due to the absence of another heavy atomic center. From the physical point of view, the single-center theorem reflects the nature of the perturbation of the otherwise highly symmetric Coulomb MO wave function by the spin-orbit interaction. We have chosen methane for the numerical illustration. Two highly distorted geometries were chosen which might be regarded as arising in highly excited vibrational states of the molecule. None of the angles were changed in comparison with the symmetric geometry of methane but the bond lengths were varied by 0.1 Å for the first geometry chosen and by 0.2 Å for the second one.

The SDE-RHF results for these two geometries are collected in Table V. One sees that even for the most distorted second geometry the reduction of the total E_{pv} against the ''normal'' SDE-RHF value of about $10^{-20}E_h$ is between 2 and 4 orders of magnitude. A similar statement is valid for the CIS-RHF results, Table VI. However, while the relative reduction of the total E_{pv} is again large and the values obtained must again be considered as negligible compared to the scale of typical values for the CIS-RHF, the absolute

TABLE V. Methane: SDE-RHF values of $E_{pv}/10^{-25}\,E_h$ (note the order of magnitude) for two geometries. Bond lengths for geometry I: $CH_1-1.1$ Å, $CH_2-1.2$ Å, $CH_3-1.3$ Å, $CH_4-1.4$ Å. Bond lengths for geometry II: $CH_1-0.7$ Å, $CH_2-0.9$ Å, $CH_3-1.1$ Å, $CH_4-1.3$ Å.

Geometry	Atom	6-31G**	D95**	TZ**	(10*s*,6*p*;1*d*)
I	C	−0.066	0.002	0.248	−0.001
	H_1	−0.004	0.011	−0.048	−0.067
	H_2	0.018	0.010	0.136	0.164
	H_3	−0.034	−0.054	−0.117	−0.130
	H_4	0.017	0.017	0.032	0.033
	total	−0.069	−0.014	0.251	−0.001
II	C	−15.262	58.720	1157.144	837.415
	H_1	5.016	6.689	3.883	−0.033
	H_2	−6.190	−7.111	−2.259	1.994
	H_3	3.133	3.525	3.952	−1.036
	H_4	−0.667	−1.365	−1.548	0.708
	total	−13.97	60.458	1161.17	839.048

CIS-RHF value of the E_{pv} for the single carbon atom in methane reaches the scale of typical SDE-RHF values.

We present these results for methane here, as there seems to be no previous numerical analysis of the single-center theorem and also because of the fundamental nature of this hydrocarbon molecule. However, it should be made clear that the results in Tables V and VI cannot be understood as definitive numerical values for the corresponding parity violating potentials in methane. This is clear from the lack of convergence with basis set size as well as with method. It is also clear that the single-center ''theorem'' for SDE-RHF in the case of CIS-RHF is reflected as a relatively weak rule by still rather small values of E_{pv} although much larger than with SDE-RHF. These might still increase with further improved calculations, thus opening the possibility to look for the corresponding effects from parity violation by a spectroscopic experiment.[46]

H. Alanine

L-alanine (in the zwitterionic structure shown in Fig. 15) is an example of a relatively large, biologically important molecule for which the magnitude of E_{pv} might perhaps play a role in evolutionary homochiral selection[43–45] although this should not be viewed too naively. Alanine also possesses kinetically stable enantiomers of C_1 point symmetry. Because of its much greater structural complexity, the chiral properties for *L*-alanine are not expected to be as simple as for the molecules considered before and three qualitatively different areas of E_{pv} behavior around each of functional groups are foreseen. The geometry of *L*-alanine used in our work is the same as in Refs. 16–19, 31, and 32 and corresponds the neutron scattering data, obtained in Ref. 96. The electronic potential for *L*-alanine is plotted in Fig. 16 as a function of the angle formed by the carboxylate plane and

TABLE VI. Methane: CIS-RHF values of $E_{pv}/10^{-25}\,E_h$ (note the order of magnitude) for two geometries. Bond lengths for geometry I: $CH_1-1.1$ Å, $CH_2-1.2$ Å, $CH_3-1.3$ Å, $CH_4-1.4$ Å. Bond lengths for geometry II: $CH_1-0.7$ Å, $CH_2-0.9$ Å, $CH_3-1.1$ Å, $CH_4-1.3$ Å.

Geometry	Atom	6-31G**	D95**	TZ**	(10*s*,6*p*;1*d*)
I	C	1737.174	−312.765	−2298.618	−123.412
	H_1	2.435	3.158	7.372	3.581
	H_2	0.689	−9.041	−0.011	0.538
	H_3	0.501	0.763	0.007	4.286
	H_4	0.414	−3.500	−5.896	0.236
	total	1741.21	−321.385	−2297.15	−114.771
II	C	10 629.506	6173.423	−7515.298	−3613.838
	H_1	−3.490	19.329	−2.799	0.627
	H_2	−49.423	−59.077	8.216	−4.517
	H_3	25.842	20.257	5.222	10.200
	H_4	−21.675	−17.919	−3.343	−9.491
	total	10 580.800	6136.010	−7508.000	−3617.02

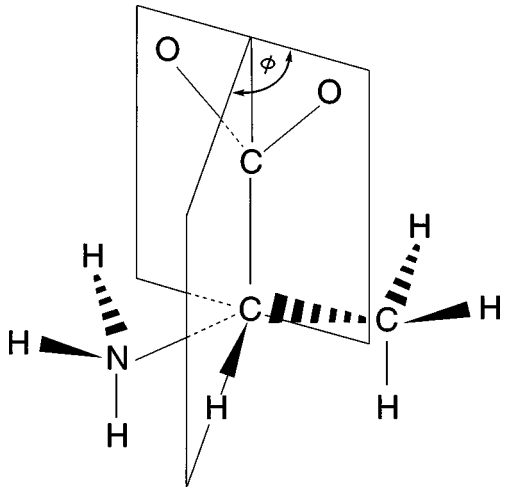

FIG. 15. The geometry of *L*-alanine used in our work is the same as in Refs. 16–19, 31, and 32 and corresponds to the neutron scattering data (Ref. 96). The torsional angle ϕ is formed by the carboxylate plane and the C_α–CO_2^-–H plane.

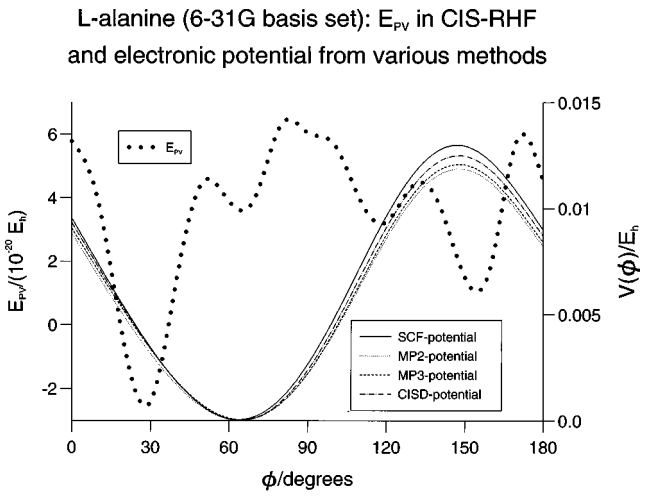

FIG. 16. *L*-alanine. Total values of E_{pv} within the CIS-RHF formalism are shown as functions of dihedral angle, as defined in Fig. 15, for the 6-31G basis set. The electronic potential $V(\phi)$ is calculated for SCF (full line), MP2 (dotted line), MP3 (dashed line), and CISD (dashed/dotted line) methods. The qualitative behavior of the total E_{pv} reflects the complicated structure of *L*-alanine better than the SDE-RHF results and has no pseudo-sinusoidal character. The changes in the E_{pv} dependence on the dihedral angle occur almost through steps of 30°, as it is expected from the relative position of the functional groups in *L*-alanine.

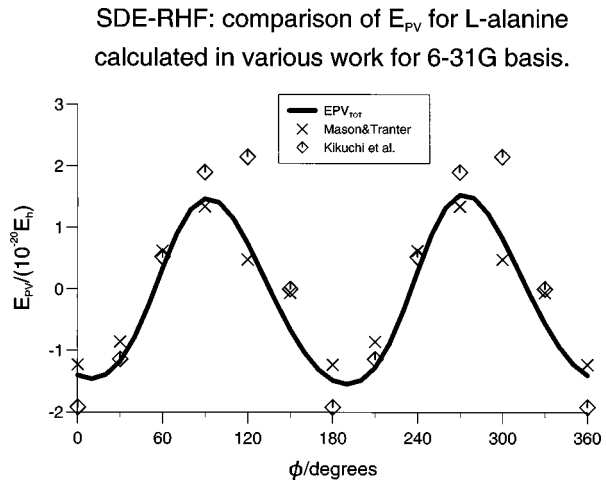

FIG. 17. *L*-alanine. Dependence of the total E_{pv} on the dihedral angle between the carboxylate plane and the plane formed by the C_α–H group and C_α–CO_2^- bond, is compared for the SDE-RHF results at the 6-31G level, obtained in this work (thick solid line) in the work by Mason and Tranter (Ref. 17) (crosses) and in the work by Kikuchi *et al.* (Refs. 31 and 32) (squares).

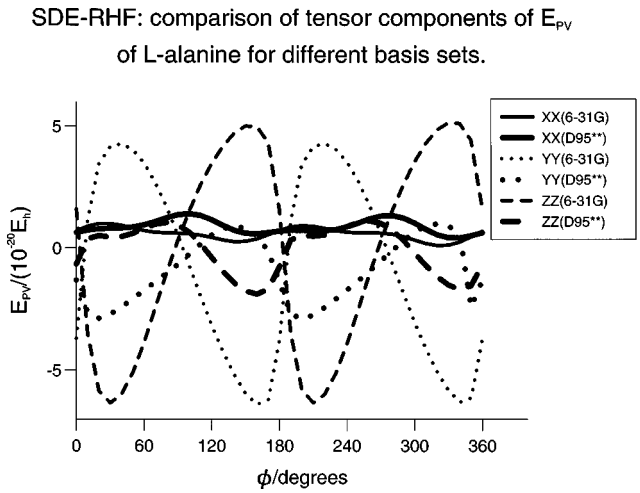

FIG. 18. *L*-alanine. Dependences of the diagonal tensor components E_{pv}^{xx} (solid lines), E_{pv}^{yy} (dotted lines), and E_{pv}^{zz} (dashed lines) on the dihedral angle between the carboxylate plane and the plane, formed by the C_α–H group and C_α–CO_2^- bond, are compared for the SDE-RHF results, obtained in this work from two different basis sets: 6-31G and D95**.

the C_α–CO_2^-–H plane. The data for these potential functions are obtained with the 6-31G basis set at SCF, MP2, MP3, and CISD levels of theory. All four functions are in qualitative agreement with each other. We shall investigate E_{pv} as a function of the torsional angle within the SDE-RHF and the CIS-RHF approaches.

We have systematically investigated the dependence of the total E_{pv} for *L*-alanine on the basis set within the SDE-RHF approach and reproduced earlier results.[16–19,31,32]

As far as the previous work is concerned, we found that our results for the 6-31G basis set are essentially the same as the results of the earlier work with the same basis set.[16–19] Figure 17 illustrates this statement. Minor differences up to about 20% can be attributed to the possible differences in the evaluations of the electrostatic potentials for spin-orbit coupling as discussed above.

While the total E_{pv}, obtained in previous work and in our work for different basis sets, shows little deviations from pseudo-sinusoidal behavior and never shows differences in sign, the diagonal tensor components E_{pv}^{ii}, $i=x,y,x$, calculated for 6-31G and DZ** basis sets show opposite signs, keeping though the zeros of the E_{pv} approximately at the same angles. This is shown in Fig. 18.

The next step is to verify whether enlarging and improving the basis set affects the overall E_{pv} behavior for *L*-alanine in the SDE-RHF approach. We have taken the same sequence of the basis sets as for small molecules arriving in the end to atomic basis sets which are the most extended bases at our disposal. Table VII shows the E_{pv} values obtained within the SDE-RHF approach for *L*-alanine. Our results are close to those obtained by Mason and Tranter[17] and we rule out the contradictory results by Kikuchi *et al.*[31] for a family of special basis sets. But the latter conclusion is valid only within the SDE-RHF approach and must be carefully reconsidered at the CIS-RHF level.

The CIS-RHF calculations made on *L*-alanine utilized the same geometry as SDE-RHF evaluations. The results are shown in the last column of Table VII. The absolute value of E_{pv} at its maximum is a factor of 4 larger with CIS-RHF than with SDE-RHF. The qualitative behavior of the total E_{pv} for *L*-alanine calculated by CIS-RHF is also distinctly different from the SDE-RHF results. E_{pv} no longer exhibits the pseudo-sinusoidal (rotamerlike) dependence on the rotation angle. At the same time the character of the changes of the values of the total E_{pv} calculated in CIS-RHF corresponds more to the intuitive view of the effects of the presence of the different functional groups in the *L*-alanine molecule as illustrated in Fig. 16. On the other hand, the smaller oscillations in $E_{pv}(\phi)$ cannot yet be considered definitive, because these first results show a relatively slow, not quite satisfactory convergence for the 250 CIS excited states, used for the perturbation theory. The latter number of CIS excited states is the technical limitation of GAUSSIAN92/94. The character of the weak convergence of the CIS-RHF perturbation theory is shown in Fig. 19, which illustrates that even at 250 CIS excited states some of the highly excited states give still appreciable contribution to the overall value of the E_{pv}.

IV. DISCUSSION AND CONCLUSIONS

(i) The new CIS-RHF approach to electroweak quantum chemistry has been implemented both analytically and numerically and leads to a change of the order of magnitude of the total parity violating potential E_{pv}. The question whether the old SDE-RHF formalism is adequately quantifying the molecular E_{pv} has been raised already by Hegstrom *et al.* ''... but what is very surprising is that the calculated values are much smaller than expected on the basis of scaling arguments alone, which predict ... $10^{-16}E_h$ for twisted ethylene and $10^{-14}E_h$ for dialkyl sulphide'' (p. 2339, Ref. 12). The new CIS-RHF formalism provides $10^{-19}E_h$ for the total E_{pv} and $10^{-18}E_h$ for the diagonal tensor components E_{pv}^{ii} for hydrogen peroxide, which is certainly nearer to the truth but the scaling arguments with $E_{pv}\sim G_F Z^{4.5}\alpha^3$ (from Ref. 12 with modification to Z dependence obtained in our work) still suggest further improvement.

TABLE VII. *L*-Alanine: SDE-RHF values of $E_{pv}/10^{-20}\,E_h$ for various basis sets and various torsion angles, compared to CIS-RHF results [last column, 6-31 G, not fully converged, for further CIS-RHF results see Table C17 in the PAPS supplement (Ref. 76)].

Angle	6-31G	6-31G**	D95	D95**	TZ	TZ**	(10*s*,6*p*;1*d*)	CIS-RHF
0°	−1.403	−1.067	−1.660	−1.346	−1.431	−1.405	−1.321	5.701
10°	−1.462	−1.072	−1.827	−1.533	−1.656	−1.670	−1.636	4.118
20°	−1.392	−1.023	−1.843	−1.584	−1.737	−1.773	−1.781	−0.695
30°	−1.175	−0.881	−1.655	−1.458	-1.610	−1.645	−1.670	−2.664
40°	−0.794	−0.601	−1.256	−1.129	−1.230	−1.245	−1.260	1.602
50°	−0.266	−0.177	−0.671	−0.614	−0.610	−0.601	−0.593	4.685
60°	0.335	0.334	0.021	0.002	0.156	0.180	0.207	3.824
70°	0.892	0.825	0.708	0.675	0.920	0.944	0.974	3.800
80°	1.292	1.188	1.283	1.249	1.532	1.550	1.560	6.616
90°	1.467	1.343	1.663	1.650	1.886	1.896	1.871	5.839
100°	1.406	1.265	1.792	1.811	1.934	1.937	1.874	5.864
110°	1.144	0.975	1.647	1.695	1.690	1.690	1.606	3.885
120°	0.740	0.547	1.252	1.323	1.230	1.239	1.165	3.120
130°	0.264	0.076	0.686	0.784	0.659	0.694	0.664	4.473
140°	−0.218	−0.347	0.005	0.196	0.007	0.143	0.173	3.942
150°	−0.660	−0.674	−0.548	−0.347	−0.462	−0.365	−0.282	1.467
160°	−1.032	−0.900	−1.068	−1.170	−0.911	−0.811	−0.698	1.519
170°	−1.312	−1.043	−1.478	−1.447	−1.272	−1.197	−1.085	6.264
180°	−1.485	−1.130	−1.765	−1.622	−1.551	−1.524	−1.443	4.373

(ii) The converged numerical results obtained here for hydrogen peroxide show the unexpectedly great difference of E_{pv} values calculated in the CIS-RHF framework and in the SDE-RHF framework, about 20 times larger in the CIS-RHF formalism. The maximum value obtained for hydrogen peroxide is in the CIS-RHF framework $3.661\times10^{-19}E_h$ (DZ** basis set) which amounts to an energy difference $\Delta E_{pv} = 7.322\times10^{-19}E_h$ between the ground states of enantiomers of this light molecule in zero external field. Molecules, containing atoms with greater nuclear charge *Z*, may have an enantiomeric energy difference corresponding to perhaps a few Hz due to the $Z^{3+\delta}$ law of amplification of E_{pv}.

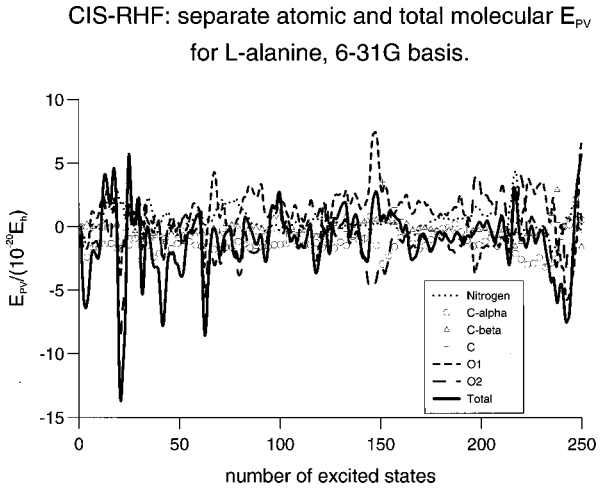

FIG. 19. *L*-alanine. For CIS-RHF formalism, the total molecular E_{pv} (solid line) is plotted together with separate atomic contributions into E_{pv} (see figure legend for specification of graphs). The figure illustrates the relatively slow convergence of the series of the perturbation theory for E_{pv} of *L*-alanine in the framework of the CIS-RHF theory for the maximal number (250) of the excited CIS states, used for the calculation. The high density of electronic states, which is about $188E_h^{-1}$ for *L*-alanine at the 6-31G level in this energy range, 5.3 times larger than that for hydrogen peroxide, suggests that the strong convergence of the perturbation theory for *L*-alanine might be formally reached somewhere at 1200 or 1300 CIS-excited states included in calculation.

(iii) As known previously and reproduced here the total E_{pv} shows ''strange'' zeros at chiral geometries. We have provided here an understanding of this phenomenon by the analysis of the diagonal tensor components of E_{pv}. The analysis revealed that each of the diagonal tensor components E_{pv}^{ii} strictly follows the symmetry of a molecule and is generally different from zero at chiral conformations both in the CIS-RHF and in the SDE-RHF formalisms. We have presented results on the systematic dependence of parity violating potentials on the molecular geometry for H_2O_2, H_2S_2, alanine, and further examples. The tensor contributions E_{pv}^{ii} have always definite sign within the given conformational range and they are fully characterized by the symmetry properties of the excited states used for perturbation of the ground state. Each of the tensor components is described by a self-conjugate operator and is therefore an independent observable. The contributions of these tensor components are sometimes another order of magnitude higher than the total E_{pv} and are of the order of $10^{-18}E_h$ even for hydrogen peroxide.

(iv) The packages of FORTRAN routines ENWEAK/RHFSDE-93 and ENWEAK/RHF-CIS-94 (see Appendix A in the PAPS supplement[76]), which have been developed for this work, allow easy change of the basis set and include by default the data for the basis sets used in this work. They run in combination with common *ab initio* MO programs, in current implementation with GAUSSIAN94/92. Both packages use the electron–nucleon weak interaction but SDE-RHF and CIS-RHF wave functions, respectively. The SDE-RHF code for E_{pv} takes no more than a few minutes of CPU time for a DEC Alpha or an IBM/RS to get one value of E_{pv} even for large basis sets. Due to the much more complicated structure of the CIS wave functions for excited states, the current version of our CIS-RHF code is progressively more expensive and slow with an increase of the basis set and of the number

of the excited states included in perturbation theory (by about a factor of 30 for DZ** basis set and frozen core CIS).

(v) For all SDE-RHF evaluations we used 6-31 G and 6-31G**, DZ and DZ**, TZ and TZ**, and $(10s,6p;1d)$ basis sets. The detailed SDE-RHF evaluations with these basis sets were carried out for small molecules in distorted structures: C_2H_2, C_2H_4, C_2H_6, N_2O_4, and CH_4. Including polarization functions allowed us to systematically recover hydrogen contributions. They have been found to be a few orders of magnitude smaller than those from heavy atoms for both the CIS-RHF and the SDE-RHF formalisms.

(vi) Our systematic investigation of the effects of nuclear charge Z on parity violating potential E_{pv} in molecules leads to a quantitative $Z^{3+\delta}$ amplification law in the CIS-RHF formalism with $\delta \approx 1.5$. However, in addition we found that this amplification is to some extent counteracted by larger bond distances in heavy molecules, for which the comparison of C_2H_4 and N_2O_4 provides an excellent illustration. Of course, further details of electronic structure can play an important role as well.

At the present stage, we cannot claim that the results of our extended CIS-RHF calculation provide definitive numerical results for E_{pv}, not even for the relatively simple molecules considered here. However, a firm summarizing conclusion from the present investigation (see also Ref. 48) is clearly that the parity violating potentials are frequently more than an order of magnitude larger than previously calculated on the basis of the SDE-RHF formalism. This provides considerable stimulus to our experimental efforts towards measuring ΔE_{pv} between enantiomers.[38–42] An important step towards such experiments has recently been taken by providing the first rotationally resolved and analyzed optical spectra of chiral molecules.[97,98]

The change of the order of magnitude of the predicted E_{pv} in combination with our finding that the total E_{pv} is a sum of three components E_{pv}^{xx}, E_{pv}^{yy}, E_{pv}^{zz}, which develop independently and with independent sign in calculations, leads to the conclusion that previous SDE-RHF results on E_{pv} of aminoacids and sugars[16,17,28,29] are uncertain even with respect to the sign. Therefore the previous claim that *L*-amino acids seem to be systematically more stable than *D*-amino acids and *D*-sugars more stable than *L*-sugars must be viewed with considerable skepticism. Even if one accepts a possible (but not necessary) connection between the biochemical evolution of homochirality and the effect arising from E_{pv} in molecules,[43–45] the latter must be established with reasonable certainty on magnitude and sign for specific systems (both potential minima and transition structures) before claiming any specific connection. On the other hand, it is also not justified to reject any possible connections because of the smallness of E_{pv}. As we have argued,[99] because of the richness of ''biochemical space'' to be explored in evolution and because of the complexity of the kinetics in living systems, extremely small variations of parity violating potentials would possibly channel the kinetic systems into completely different portions of biochemical space. Thus, even if enantiomeric, very complex biochemical systems show near mirror symmetry, small violations of this symmetry would prevent the near symmetry from ever being actually realized in a practical biochemical system. At present we consider the question of the *de facto*[39] (i.e., by chance) versus *de lege*[39] (i.e., deterministic) selection of a specific homochiral biochemical system to be completely open. Abdus Salam has even proposed an *abiotic de lege* selection of homochirality.[36,37]

Further theoretical and experimental insights into parity violating potentials in polyatomic molecules may help to resolve this question in the future. We have argued that, in principle, in the presence of a proven bias, the *de lege* hypothesis would be the ''better guess,'' but a very weak guess, indeed, with very little certainty at present.[45] The trend towards larger ΔE_{pv} in the present calculations might also be favorable to possible laboratory tests of the effect of ΔE_{pv} on the evolution of biochemical homochirality[43] if ever laboratory experiments on the evolution of life become available.

In a completely different context the present effort towards quantitative calculations of E_{pv} in molecules may prove useful as well. If quantitative measurements of E_{pv} become available to be compared with truly accurate calculations of the same quantity from electroweak quantum chemistry, then some fundamental tests of the electroweak theory and the standard model in particle physics might become feasible in the realm of molecular physics. While such a result is surely still far ahead, our work is intended to opening routes towards such investigations.

ACKNOWLEDGMENTS

We enjoyed help from and discussions with R. Berger, D. Luckhaus, U. Schmitt, J. Stohner, and M. Suhm as well as discussions with J. Chela-Flores and H. F. Schaefer III, and useful remarks by J. Tomasi and R. McWeeny during a seminar on electroweak grounds of the formalism by A.B. (in Pisa, 1993). Our work is supported financially by the Schweizerischer Nationalfonds (in part by Chiral II) and by the ETH-Zurich. This paper is dedicated to the memory of Abdus Salam and Friedrich Hund, who influenced our thinking at earlier stages of our life by discussions and teaching and who profoundly influenced the theory of parity violation and chirality.

[1] F. Hund, Z. Phys. **43**, 805 (1927); see also the discussion by R. Janoschek, ''Theories on the origin of biomolecular homochirality,'' in *Chirality*, edited by R. Janoschek (Springer-Verlag, Berlin, 1991), p. 18.
[2] T. D. Lee and C. N. Yang, Phys. Rev. **104**, 254 (1956).
[3] C. S. Wu, E. Ambler, R. W. Hayward, D. D. Hoppes, and R. P. Hudson, Phys. Rev. **105**, 1413 (1957).
[4] S. L. Glashow, Nucl. Phys. **22**, 579 (1961).
[5] S. Weinberg, Phys. Rev. Lett. **19**, 1264 (1967).
[6] A. Salam, in *Proceedings of the Eighth Nobel Symposium*, edited by N. Svartholm (Amkvist and Wiksell, Stockholm, 1968), p. 367.
[7] D. W. Rein, J. Mol. Evol. **4**, 15 (1974).
[8] V. S. Letokhov, Phys. Lett. **A53**, 275 (1975).
[9] B. Ya. Zel'dovich, Sov. Phys. JETP **9**, 682 (1959); B. Ya. Zel'dovich, D. B. Saakyan, and I. I. Sobel'man, JETP Lett. **25**, 94 (1977).
[10] R. A. Harris and L. Stodolski, Phys. Lett. **B78**, 313 (1978); J. Chem. Phys. **73**, 3862 (1980).
[11] D. W. Rein, R. A. Hegstrom, and P. G. H. Sandars, Phys. Lett. **A71**, 499 (1979).
[12] R. A. Hegstrom, D. W. Rein, and P. G. H. Sandars, J. Chem. Phys. **73**, 2329 (1980).
[13] S. F. Mason and G. E. Tranter, Chem. Phys. Lett. **94**, 34 (1983).

[14] S. F. Mason and G. E. Tranter, J. Chem. Soc. Chem. Commun. **1983**, 117.
[15] S. F. Mason, Int. Rev. Phys. Chem. **3**, 217 (1983); Nature (London) **314**, 400 (1985).
[16] S. F. Mason and G. E. Tranter, Mol. Phys. **53**, 1091 (1984).
[17] S. F. Mason, F. R. S. , and G. E. Tranter, Proc. R. Soc. London, Ser. A **397**, 45 (1985).
[18] G. E. Tranter, Chem. Phys. Lett. **115**, 286 (1985).
[19] G. E. Tranter, Mol. Phys. **56**, 825 (1985).
[20] G. E. Tranter, Chem. Phys. Lett. **120**, 83 (1985); Nature (London) **318**, 172 (1985).
[21] G. E. Tranter, J. Chem. Soc. Chem. Commun. **1986**, 60; Nachr. Chem., Tech. Lab. **34**, 866 (1986).
[22] G. E. Tranter and A. J. MacDermott, Chem. Phys. Lett. **130**, 120 (1986).
[23] G. E. Tranter, Chem. Phys. Lett. **135**, 279 (1987).
[24] A. J. MacDermott, G. E. Tranter, and S. B. Indoe, Chem. Phys. Lett. **135**, 159 (1987).
[25] A. J. MacDermott and G. E. Tranter, Chem. Phys. Lett. **163**, 1 (1989).
[26] A. J. MacDermott and G. E. Tranter, Croat. Chem. Acta **62**, 165 (1989).
[27] A. J. MacDermott and G. E. Tranter, in *Symmetries in Science IV, Biological and Biophysical Systems*, edited by B. Gruber and J. H. Yopp (Plenum, New York, 1990), p. 67.
[28] A. J. MacDermott, G. E. Tranter, and S. J. Trainor, Chem. Phys. Lett. **194**, 152 (1992).
[29] G. E. Tranter, A. J. MacDermott, R. E. Overill, and P. J. Speers, Proc. R. Soc. London, Ser. A **436**, 603 (1992).
[30] A. J. MacDermott, in *Chemical Evolution: Origin of Life*, edited by C. Ponnamperuma and J. Chela-Flores, (DEEPAK Hampton, 1993), p. 85.
[31] O. Kikuchi and H. Wang, Bull. Chem. Soc. Jpn. **63**, 2751 (1990).
[32] O. Kikuchi, H. Wang, T. Nakano, and K. Morihashi, J. Mol. Struct. **205**, 301 (1990).
[33] A. L. Barra, J. B. Robert, and L. Wiesenfeld, Phys. Lett. A **115**, 443 (1986).
[34] A. L. Barra, J. B. Robert, and L. Wiesenfeld, Europhys. Lett. **5**, 217 (1988).
[35] L. Wiesenfeld, Mol. Phys. **64**, 739 (1988).
[36] A. Salam, J. Mol. Evol. **33**, 105 (1991).
[37] A. Salam, Phys. Lett. B **288**, 153 (1992).
[38] M. Quack, Chem. Phys. Lett. **132**, 147 (1986).
[39] M. Quack, Angew. Chem. **101**, 588 (1989); Angew. Chem. Int. Ed. Engl. **28**, 571 (1989).
[40] M. Quack, J. Mol. Struct. **292**, 171 (1993).
[41] M. Quack, Chem. Phys. Lett. **231**, 421 (1994).
[42] M. Quack, in *Femtosecond Chemistry*, Proc. Berlin Femtosecond Chemistry, Berlin, 1993, edited by J. Manz and L. Wöste (Verlag Chemie, Weinheim, 1994), p. 781.
[43] D. K. Kondepudi and G. W. Nelson, Phys. Rev. Lett. **50**, 1023 (1983).
[44] D. K. Kondepudi and G. W. Nelson, Nature (London) **314**, 438 (1985).
[45] M. Quack, J. Mol. Struct. **347**, 245 (1995).
[46] M. J. M. Pepper, I. Shavitt, P. von R. Schleyer, M. N. Glukhovtsev, R. Janoschek, and M. Quack, J. Comput. Chem. **16**, 207 (1995).
[47] M. Quack, J. Chem. Soc. Faraday Disc. **99**, 389 (1994).
[48] A. A. Bakasov, T.-K. Ha, and M. Quack, in *Proceedings of the Fourth Trieste Conference on Chemical Evolution: Physics of the Origin and Evolution of Life*, edited by J. Chela-Flores and F. Raulin (Kluwer Academic, Dordrecht, 1996), p. 287.
[49] I. B. Khriplovich, *Parity Nonconservation in Atomic Phenomena* (Gordon and Breach, Philadelphia, 1991).
[50] E. D. Commins and P. H. Bucksbaum, *Weak Interactions of Leptons and Quarks* (Cambridge University Press, Cambridge, 1983).
[51] N. N. Bogolubov and D. V. Shirkov, *Quantum Fields* (Benjamin/Cummings, Reading, MA, 1983).
[52] R. A. Hegstrom, J. Mol. Struct. **232**, 17 (1991).
[53] R. A. Hegstrom, J. P. Chamberlein, K. Seto, and R. G. Watson, Am. J. Phys. **56**, 1086 (1988).
[54] M. A. Bouchiat and C. C. Bouchiat, Rep. Prog. Phys. **60**, 1351 (1997).
[55] M. G. Kozlov and L. N. Labzowski, J. Phys. B **28**, 1933 (1995).
[56] H. M. Quiney, H. Skaane, and I. P. Grant, J. Phys. B **30**, L829 (1997).
[57] M. G. Kozlov, A. V. Titov, N. S. Mosyagin, and P. V. Souchko, Phys. Rev. A **56**, R3326 (1997).
[58] N. N. Bogolubov and D. V. Shirkov, *Introduction to the Theory of Quantized Fields*, (Wiley, New York, 1980).
[59] B. N. Taylor and E. R. Cohen, J. Res. Natl. Inst. Stand. Technol. **95**, 497 (1990).
[60] E. R. Cohen and B. N. Taylor, The Fundamental Physical Constants, Phys. Today August 1993, Part 2, BG9.
[61] A. Salam (private communication).
[62] M. A. Bouchiat and C. C. Bouchiat, J. Phys. **35**, 899 (1974).
[63] M. A. Bouchiat and C. C. Bouchiat, J. Phys. **36**, 493 (1975).
[64] F. Curtis Michel, Phys. Rev. B **133**, B329 (1964).
[65] F. Curtis Michel, Phys. Rev. B **138**, B408 (1965).
[66] J. C. Slater, *Quantum Theory of Matter*, 2nd ed. (McGraw Hill, New York, 1968).
[67] A. Szabo and N. S. Ostlund, *Modern Quantum Chemistry* (McGraw-Hill, New York, 1989).
[68] R. McWeeny, J. Chem. Phys. **42**, 1717 (1965).
[69] P. Schmelcher, L. S. Cederbaum, and U. Kappes, in *Conceptual Trends in Quantum Chemistry*, edited by E. S. Kryachko and J. L. Calais (Kluwer Academic, Dordrecht, 1994), p. 1.
[70] B. A. Hess, C. M. Marian, and S. D. Peyerimhoff, in *Modern Electronic Structure Theory, Part I*, edited by D. R. Yarkony (World Scientific, Singapore, 1995), p. 152.
[71] A. L. Barra and J. B. Robert, Mol. Phys. **88**, 875 (1996).
[72] T. R. Furlani and H. F. King, J. Chem. Phys. **82**, 5577 (1985).
[73] I. I. Sobelman, *Introduction to the Theory of Atomic Spectra* (Pergamon, Oxford, 1972).
[74] B. Edlen, *Atomic Spectra*, *Encyclopedia of Physics*, (Springer-Verlag, Berlin, 1964), Vol. XXVII, p. 80.
[75] J. B. Foresman, M. Head-Gordon, J. A. Pople, and M. J. Frisch, J. Phys. Chem. **96**, 135 (1992).
[76] See AIP Document No. PAPS JCPSA6-109-303832 for 31 pages of Appendices. Order by PAPS number and journal reference from American Institute of Physics, Physics Auxillary Publication Service, 500 Sunnyside Boulevard, Woodbury, NY 11797-2999. Fax: 516-576-2223, e-mail: paps@aip.org. The price is $1.50 for each microfiche (98 pages) or $5.00 for photocopies of up to 30 pages and $0.15 for each additional page over 30 pages. Airmail additional. Make checks payable to the American Institute of Physics.
[77] X. Luo and T. R. Rizzo, J. Chem. Phys. **93**, 8620 (1990).
[78] W. B. Olson, R. H. Hint, B. W. Young, A. G. Maki, and J. W. Brault, J. Mol. Spectrosc. **127**, 12 (1988).
[79] F. Masset, L. Lechuga-Fossat, J.-M. Flaud, C. Camy-Peyret, J. W. Johns, B. Carli, M. Carlotti, L. Fusina, and A. Trombetti, J. Phys. (France) **49**, 1901 (1988).
[80] T. M. Ticich, T. R. Rizzo, H.-R. Dübal, and F. F. Crim, J. Chem. Phys. **84**, 1508 (1986).
[81] B. Kuhn, T. Rizzo, D. Luckhaus, M. Quack, and M. Suhm (unpublished).
[82] M. J. Frisch *et al.*, GAUSSIAN 92, Revision E.2 (Gaussian, Inc., Pittsburgh, PA, 1992); GAUSSIAN 94, Revision A.1 (Gaussian, Inc., Pittsburgh, PA, 1995).
[83] J. Cohen, Science **267**, 1265 (1995).
[84] J. Bada, Nature (London) **374**, 594 (1995).
[85] T. H. Dunning, Jr., J. Chem. Phys. **53**, 2823 (1970).
[86] T. H. Dunning, Jr., J. Chem. Phys. **55**, 716 (1971).
[87] S. Huzinaga, J. Chem. Phys. **42**, 1293 (1965).
[88] R. H. Hunt, R. A. Leacock, C. W. Peters, and K. T. Hecht, J. Chem. Phys. **42**, 1931 (1965).
[89] L. Keszthelyi, J. Biol. Phys. **20**, 241 (1994).
[90] S. Urban, E. Herbst, P. Mittler, G. Winnewisser, and K. M. T. Yamada, J. Mol. Spectrosc. **137**, 327 (1989).
[91] D. Luckhaus and M. Quack, Chem. Phys. Lett. **199**, 293 (1992).
[92] R. Ahlrichs and F. Keil, J. Am. Chem. Soc. **96**, 7615 (1974).
[93] C. W. Bauschlicher, Jr., A. Komornicki, and B. Roos, J. Am. Chem. Soc. **105**, 745 (1983).
[94] U. Kaldor and I. Shavitt, J. Chem. Phys. **48**, 191 (1968).
[95] T. D. Bouman and A. E. Hansen, J. Chem. Phys. **66**, 3460 (1977).
[96] M. S. Lehmann, T. F. Koetzle, and W. C. Hamilton, J. Am. Chem. Soc. **94**, 2657 (1972).
[97] A. Bauder, A. Beil, D. Luckhaus, F. Müller, and M. Quack, J. Chem. Phys. **106**, 7558 (1997).
[98] H. Hollenstein, D. Luckhaus, J. Pochert, M. Quack, and G. Seyfang, Angew. Chem. **109**, 136 (1997); Angew. Chem. Int. Ed. Engl. **36**, 140 (1997).
[99] M. Quack, Philos. Trans. R. Soc. London, Ser. A **332**, 203 (1990); see also the lecture in the Organisch-Chemisches Kolloqium ETH-Zurich, 1996. A very similar argument with just the opposite emphasis (i.e., de facto hypothesis) has recently been made by M. Bolli, R. Micura, and A. Eschenmoser, Chem. Biol. **4**, 309 (1997) (in particular p. 317 therein).